STRUCTURAL CHEMISTRY

ISSN 2053-2296

Chalcogen bonding in the solid-state structures of 1,3-bis(benzimidazoliumyl)benzene-based chalcogen-bonding donors

Tim Steinke, Elric Engelage and Stefan M. Huber*

Fakultät für Chemie und Biochemie, Ruhr-Universität Bochum, Universitätsstrasse 150, Bochum, 44801, Germany. *Correspondence e-mail: stefan.m.huber@rub.de

Received 24 August 2022
Accepted 30 November 2022

Edited by T. Roseveare, University of Sheffield, United Kingdom

Keywords: chalcogen bonding; Lewis acid; crystal structure; sigma hole; intermolecular interactions; benzimidazolium.

CCDC references: 2201758; 2201759; 2201760; 2201761

Supporting information: this article has supporting information at journals.iucr.org/c

1,3-Bis(benzimidazoliumyl)benzene-based chalcogen-bonding catalysts were previously successfully applied in different benchmark reactions. In one of those examples, *i.e.* the activation of quinolines, sulfur- and selenium-based chalcogen-bonding catalysts showed comparable properties, which is unexpected, as the selenium-containing catalysts should show superior catalytic properties due to the increased polarizability of selenium compared to sulfur. Herein, we present four crystal structures of the respective 1,3-bis(benzimidazoliumyl)benzene-based chalcogen-bonding catalyst containing sulfur (**3**^{S}) and selenium (**3**^{Se}, three forms) as Lewis acidic centres. The sulfur-containing catalyst shows weaker chalcogen bonding compared to its selenium analogue, as well as anion–π interactions. The selenium-based analogues, on the other hand, show stronger chalcogen-bonding motifs compared to the sulfur equivalent, depending on the crystallization conditions, but in every case, the intermolecular interactions are comparable in strength. Other interactions, such as hydrogen bonding and anion–π, were also observed, but in the latter case, the interaction distances are longer compared to those of the sulfur-based equivalent. The solid-state structures could not further explain the high catalytic activity of the sulfur-containing catalysts. Therefore, a comparison of their σ-hole depths from density functional theory (DFT) gas-phase calculations was performed, which are again in line with the previously found properties in the solid-state structures.

1. Introduction

Chalcogen bonding (ChB) (Aakeroy *et al.*, 2019) is defined as the attractive interaction of Lewis acidic chalcogen centres with Lewis bases and is closely related to hydrogen bonding (Doyle & Jacobsen, 2007) and halogen bonding (Cavallo *et al.*, 2016). However, chalcogen bonding is the least investigated interaction in this group. This interaction can be explained by three major contributions, again similar to hydrogen and halogen bonding: (i) charge transfer, described by an n$\rightarrow\sigma^*$-orbital interaction (Mulliken, 1952); (ii) electrostatic attraction of the lone pair of the Lewis base with an electropositive region (σ-hole) at the chalcogen (Rosenfield *et al.*, 1977); (iii) dispersion (Bleiholder *et al.*, 2006). In general, chalcogen bonding is a more directional interaction compared to hydrogen bonding, which is explained by the absence of filled *p*-orbitals at hydrogen and by the fact that the σ^*-orbital of the *R*—H bond is comprised of the 1*s* orbital on the hydrogen side. Furthermore, the interaction site is not limited to a single atom and can vary between tellurium, selenium and sulfur, which consequently allows the fine tuning of the interaction strength. Less electronegativity and easier polarization of the chalcogen leads to an increased anisotropic electron distribution and thus an enlarged electropositive region (σ-hole), as

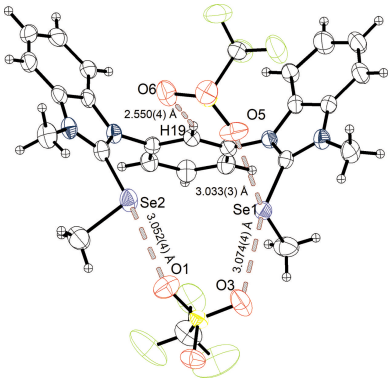

well as to a lower-lying σ*-orbital of the R—Ch bond. Hence, the strength of the chalcogen bonding increases with the atomic number of chalcogen (S < Se < Te). Another difference to hydrogen and halogen bonding is the second substituent located at the interacting atom. This interaction was observed in several solid-state systems, such as Ebselen, a synthetic organoselenium drug (Dupont *et al.*, 1990) and diphenyl diselenide with iodine (Kubiniok *et al.*, 1988). Intensive studies (Bleiholder *et al.*, 2006) and applications of the Gleiter group used chalcogen–chalcogen interactions to synthesize porous materials, such as nanotubes (Werz *et al.*, 2002), that incorporated other organic molecules like solvents (Werz *et al.*, 2004). In parallel, first applications in solution appeared as intramolecular chalcogen bonding was applied for the rigidification of intermediates to induce chirality (Fujita *et al.*, 1994; Wirth, 1995; Tiecco *et al.*, 2002). Moving from intra- to intermolecular interactions in solution, pioneering works in the field of anion recognition *via* chalcogen bonding have been performed by Gabbaï and co-workers (Zhao & Gabbaï, 2010) using charged chalcogen-bonding donors, and by Taylor and co-workers with neutral chalcogen-bonding donors (Garrett *et al.*, 2015). Extending the field of anion recognition to anion transport, the group of Matile introduced neutral dithienothiophene (DTT) chalcogen-bonding donors (Benz *et al.*, 2016), which were also employed in oligomeric fashion as transmembrane transporters in further studies (Macchione *et al.*, 2018). Furthermore, with the DTT motif, the first application of chalcogen bonding in organocatalysis was presented by the same group (Benz *et al.*, 2017). Catalytic amounts of these compounds successfully activate quinolines for their reductive hydrogenation to 1,2,3,4-tetrahydroquinoline derivatives. In halogen-bonding organocatalysis, cationic donors were often markedly more active than neutral donors (Jungbauer & Huber, 2015). Therefore, our group reported the use of cationic chalcogen-bonding donors, which contained the more Lewis acidic chalcogen selenium on a 1,3-bis(benzimidazoliumyl)benzene scaffold (Wonner *et al.*, 2017*a*). These catalysts were used in stoichiometric (Wonner *et al.*, 2017*a*) and catalytic (Wonner *et al.*, 2017*b*) activations of carbon–halide bonds. We also successfully demonstrated the catalytic activity of the same catalyst and the sulfur congener in the above-mentioned hydrogenation reaction (Wonner *et al.*, 2019*b*).

The use of cationic selenium-based Lewis acids was further extended by Wang and co-workers in the activation of carbonyl functionalities (Wang *et al.*, 2019). As the development of chalcogen-bonding catalysts moved on, tellurium-based catalysts were introduced and applied in the activation of *trans*-β-nitrostyrene (Wonner *et al.*, 2019*a*) and crotonophenone (Wonner *et al.*, 2020) for Michael reactions, as well as in the activation of a carbon–chloride bond (Steinke *et al.*, 2021) and of imines (Steinke *et al.*, 2022). Lately, hypervalent tellurium-based chalcogen-bonding donors were introduced in organocatalysis (Weiss *et al.*, 2021; Zhou & Gabbaï, 2021). Herein, we present four crystal structures of 1,3-bis(benzimidazoliumyl)benzene-based chalcogen-bonding donors with selenium and sulfur as Lewis acidic centres. Monodentate, bidentate and biaxial intermolecular chalcogen-bonding interactions are observed in these solid-state structures, which are further discussed in terms of previously observed catalytic activity. In addition, we performed DFT calculations to analyze chalcogen bonding in the absence of packing effects observed in the crystal structures of the catalyst system at hand.

2. Experimental

2.1. General remarks

Commercially available chemicals were purchased from ABCR, Alfa Aesar, Carbolution, Merck, ChemPur, Sigma–Aldrich, Roth or VWR and were used without further purification. All experiments were carried out under an inert gas atmosphere with dry solvents and flame-dried glassware using standard Schlenk techniques. Dry dichloromethane, diethyl ether and tetrahydrofuran were received from an MBRAUN MB SPS-800 solvent purification system. Solvents were distilled and dried over a 4 Å molecular sieve and finally dried on an Alox column. Other dry solvents were dried with flame-dried 4 Å molecular sieve. A Karl Fischer Titroline 7500KF trace with Honeywell Hydranal–Coulomat AD solution was used to determine residual water. Merck thin-layer chromatography (TLC) aluminium sheets (silica gel 60, F254) were used for TLC analysis. Substances were detected by fluorescence under UV light (wavelength λ = 254 nm). Column chromatography was performed with silica gel (grain size 0.04–0.063 mm, Macherey–Nagel-Si60) and distilled solvents. The solvents used as eluents with the corresponding R_F values are listed for the corresponding experiments. ^{1}H and ^{13}C NMR spectra were recorded at room temperature with a Bruker AVIII 300 spectrometer. ^{19}F NMR spectra were recorded at room temperature with a Bruker DPX-250 spectrometer and were measured proton decoupled if not further noted. ESI–MS spectra were recorded with a Bruker Esquire 6000, with the compounds dissolved in acetonitrile or methanol. EI–MS spectra were recorded on a Jeol AccuTOF. FT–IR spectra were recorded with a Shimadzu IR Affinity-IS spectrometer equipped with a Specac-Quest ATR module. The crystal structures were analysed on a Rigaku Synergy dual-source device, with a Cu microfocus sealed tube (Cu $K\alpha$) using mirror monochromators and a HyPix-6000HE Hybrid photon counting X-ray detector. The crystals were mounted in Hampton CryoLoops using GE/Bayer silicone grease. Data were recorded and reduced using *Crysalis PRO* software (Rigaku OD, 2018). The structure was solved using *WinGX* (Farrugia, 2012) in combination with *SHELXT* (Sheldrick, 2015*a*) and refined with *shelXle* (Hübschle *et al.*, 2011) and *SHELXL* (Sheldrick, 2015*b*).

2.2. Synthesis of known compounds

1,3-Bis(benzimidazolyl)benzene (Ganta & Chand, 2015) and 3,3′-dimethyl-1,1′-(1,3-phenylene)bis(1*H*-1,3-benzodiazol-3-ium) bis(trifluoromethanesulfonate), **1** (Liu *et al.*, 2019), were synthesized according to literature procedures.

Table 1
Experimental details.

Experiments were carried out at 170 K with Cu $K\alpha$ radiation using a Rigaku XtaLAB Synergy Dualflex diffractometer with a HyPix detector. H-atom parameters were constrained.

	$\mathbf{3^S}$	$\mathbf{3^{Se}}$-A	$\mathbf{3^{Se}}$-B	$\mathbf{3^{Se}}$-C
Crystal data				
Chemical formula	$C_{24}H_{24}N_4S_2^{2+}\cdot 2CF_3O_3S^-$	$C_{24}H_{24}N_4Se_2^{2+}\cdot 2CF_3O_3S^-$	$C_{24}H_{24}N_4Se_2^{2+}\cdot 2CF_3O_3S^-$	$C_{24}H_{24}N_4Se_2^{2+}\cdot 2CF_3O_3S^-\cdot 0.5C_2H_4Cl_2$
M_r	730.73	824.53	824.53	874.01
Crystal system, space group	Monoclinic, $P2_1/c$	Monoclinic, $P2_1/c$	Monoclinic, $P2_1/c$	Triclinic, $P\overline{1}$
a, b, c (Å)	7.7776 (2), 22.5823 (6), 18.2338 (5)	7.74775 (4), 13.12863 (8), 31.27496 (18)	13.8634 (4), 7.7558 (2), 29.3266 (7)	9.3672 (1), 13.3265 (2), 13.6445 (1)
α, β, γ (°)	90, 99.329 (2), 90	90, 90.6141 (5), 90	90, 94.246 (2), 90	102.515 (1), 93.231 (1), 96.198 (1)
V (Å^3)	3160.16 (15)	3181.02 (3)	3144.59 (14)	1647.49 (3)
Z	4	4	4	2
μ (mm^{-1})	3.51	4.88	4.94	5.48
Crystal size (mm)	0.13 × 0.06 × 0.03	0.29 × 0.14 × 0.08	0.03 × 0.02 × 0.01	0.19 × 0.10 × 0.08
Data collection				
Absorption correction	Multi-scan (*CrysAlis PRO*; Rigaku OD, 2018)	Gaussian (*CrysAlis PRO*; Rigaku OD, 2018)	Gaussian (*CrysAlis PRO*; Rigaku OD, 2018)	Gaussian (*CrysAlis PRO*; Rigaku OD, 2018)
T_{min}, T_{max}	0.579, 1.000	0.300, 1.000	0.900, 0.969	0.456, 1.000
No. of measured, independent and observed [$I > 2\sigma(I)$] reflections	21606, 5564, 4631	37979, 5613, 5268	28154, 5529, 4865	19605, 5795, 5307
R_{int}	0.043	0.039	0.073	0.046
$(\sin\theta/\lambda)_{max}$ (Å^{-1})	0.595	0.595	0.595	0.595
Refinement				
$R[F^2 > 2\sigma(F^2)]$, $wR(F^2)$, S	0.073, 0.205, 1.09	0.028, 0.070, 1.02	0.053, 0.142, 1.06	0.048, 0.127, 1.05
No. of reflections	5564	5613	5529	5795
No. of parameters	419	486	419	484
No. of restraints	0	0	0	28
$\Delta\rho_{max}$, $\Delta\rho_{min}$ (e Å^{-3})	0.69, −0.39	0.60, −0.78	1.21, −0.84	0.84, −0.80

Computer programs: *CrysAlis PRO* (Rigaku OD, 2018), *SHELXT* (Sheldrick, 2015*a*), *shelXle* (Hübschle *et al.*, 2011), *SHELXL2018* (Sheldrick, 2015*b*), *DIAMOND* (Putz & Brandenburg, 2014), *Mercury* (Macrae *et al.*, 2020) and *WinGX* (Farrugia, 2012).

2.3. Synthesis of new compounds

2.3.1. Precursor $\mathbf{2^S}$. A reported procedure was slightly modified for the synthesis of compound $\mathbf{2^S}$ (Wonner *et al.*, 2017*a*, 2019*b*). In a flame-dried 100 ml Schlenk flask, 1.00 g of **1** (1.57 mmol, 1.00 eq.) was added and dissolved in 30 ml dry methanol (52.3 m*M*). To the solution were added 1.00 g sulfur (3.92 mmol, 2.50 eq.) and 1.28 g Cs_2CO_3 (3.92 mmol, 2.50 eq.). The resulting suspension was stirred for 24 h under reflux. The mixture was filtered over a pad of silica, which was rinsed twice with dichloromethane (DCM). The solvents were removed under reduced pressure and the crude solid was purified by column chromatography with pentane–EtOAc (2:1 *v*/*v*) (R_F = 0.33). The solvents were removed under reduced pressure and product $\mathbf{2^S}$ was obtained as a white solid (m.p. 240 °C). Yield: 0.547 g (1.36 mmol, 87%). ^{1}H NMR (300 MHz, chloroform-*d*): δ (ppm) = 7.82–7.75 (*m*, 4H), 7.48 (*d*, *J* = 7.9 Hz, 2H), 7.36 (*t*, *J* = 7.7 Hz, 4H), 7.29–7.23 (*m*, 2H), 3.92 (*s*, 6H). ^{13}C NMR (75 MHz, chloroform-*d*): δ (ppm) = 170.30, 136.84, 132.73, 132.64, 130.36, 128.19, 127.74, 123.83 (*d*, *J* = 5.5 Hz), 110.59, 109.05, 31.48. ATR-IR: $\tilde{\nu}$ (cm^{-1}) = 3030 (*w*), 2924 (*m*), 2345 (*w*), 1736 (*m*), 1728 (*m*), 1601 (*s*), 1589 (*m*), 1476 (*s*), 1454 (*m*), 1427 (*s*), 1377 (*vs*), 1337 (*vs*), 1302 (*s*), 1265 (*s*), 1211 (*vs*), 1161 (*m*), 1144 (*m*), 1119 (*s*), 1015 (*m*), 993 (*m*), 924 (*m*), 887 (*w*), 849 (*w*), 806 (*s*), 743 (*vs*), 714 (*vs*), 692 (*vs*), 615 (*s*), 559 (*vs*), 540 (*m*), 471 (*s*), 432 (*m*), 420 (*vs*). EI–MS (70 eV): *m*/*z*(+) = 402.2 $[M]^+$, 369.2 $[M - S]^+$.

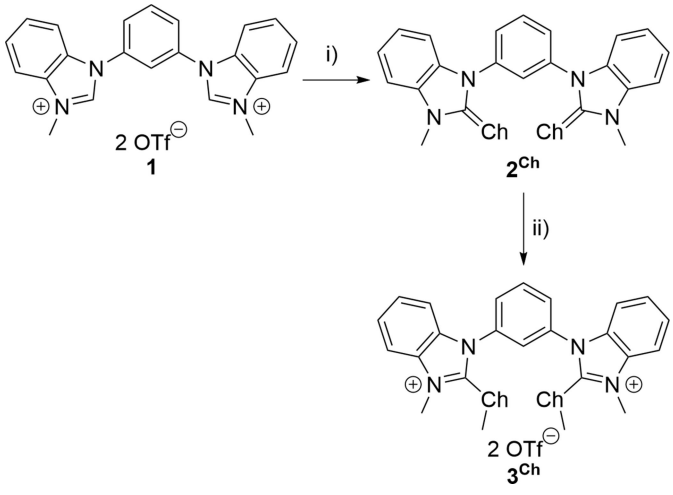

Figure 1
Synthesis of the chalcogen-bonding catalysts investigated in this report. (i) Ch (2.50 eq.), Cs_2CO_3 (2.50 eq.), MeOH, reflux, 3 d ($\mathbf{2^S}$ = 87%; $\mathbf{2^{Se}}$ = 60%); (ii) MeOTf (2.50 eq.), DCM, room temperature, 24 h ($\mathbf{3^S}$ = 86%; $\mathbf{3^{Se}}$ = 92%) (Ch = S or Se) (Wonner *et al.*, 2019*b*).

2.3.2. Precursor $\mathbf{2^{Se}}$. A reported procedure was slightly modified for the synthesis of compound $\mathbf{2^{Se}}$ (Wonner *et al.*, 2017*a*, 2019*b*). In a flame-dried 100 ml Schlenk flask, 0.50 g of **1** (0.783 mmol, 1.00 eq.) was added and dissolved in 15 ml dry

methanol (52.3 m*M*). To this solution were added 0.155 g selenium (1.96 mmol, 2.50 eq.) and 0.638 g Cs_2CO_3 (1.96 mmol, 2.50 eq.). The resulting suspension was stirred for 24 h under reflux. The mixture was filtered over a pad of silica, which was rinsed twice with DCM. The solvents were removed under reduced pressure and the crude solid was purified by column chromatography with pentane–EtOAc (1:1 *v*/*v*) (R_F = 0.59). The solvents were removed under reduced pressure and product **2**^{Se} was obtained as a white solid (m.p. = 266 °C). Yield: 0.234 g (0.471 mmol, 60%). ^{1}H NMR (400 MHz, acetonitrile-d_3): δ (ppm) = 7.86–7.75 (*m*, 4H), 7.48 (*d*, *J* = 7.9 Hz, 2H), 7.36 (*t*, *J* = 7.7 Hz, 4H), 7.31–7.24 (*m*, 2H), 3.92 (*s*, 6H). ^{13}C NMR (75 MHz, chloroform-*d*): δ (ppm) = 167.36, 137.58, 133.97, 133.67, 130.52, 128.97, 128.97, 124.29 (*d*, *J* = 1.2 Hz), 111.31, 109.58, 33.58. ATR-IR: $\tilde{\nu}$ (cm^{-1}) = 3053 (*w*), 2922 (*m*), 2853 (*w*), 1726 (*w*), 1601 (*m*), 1589 (*m*), 1493 (*m*), 1474 (*s*), 1456 (*m*), 1425 (*m*), 1375 (*s*), 1333 (*vs*), 1306 (*s*), 1298 (*s*), 1263.37 (*s*), 1211 (*s*), 1161 (*m*), 1144 (*m*), 1121 (*s*), 1084 (*s*), 1015 (*m*), 991 (*m*), 874 (*m*), 853 (*m*), 808 (*s*), 802 (*s*), 745 (*vs*), 709 (*s*), 691 (*s*), 675 (*m*), 646 (*m*), 617 (*m*), 592 (*m*), 557 (*s*), 534 (*m*), 469 (*m*), 430 (*m*). EI–MS (70 ev): *m*/*z* = 417.10 [*M* − Se]$^+$.

2.3.3. Chalcogen-bonding donor 3^S. A reported procedure was slightly modified for the synthesis of compound **3**^{S} (Wonner *et al.*, 2017*a*, 2019*b*). To a flame-dried 50 ml Schlenk flask was added 0.400 g of **2**^{S} (0.984 mmol, 1.00 eq.) dissolved in 15 ml dry DCM (66.3 m*M*). Afterwards, 0.281 ml methyl trifluoromethanesulfonate (0.408 g, 2.48 mmol, 2.50 eq.) was added dropwise. The mixture was stirred for 24 h at room temperature. The solvent was removed under reduced pressure. The crude solid was washed three times with diethyl ether and three times with pentane, and then dried under high vacuum. Product **3**^{S} was obtained as a pale-yellow solid (m.p. = 222 °C). Yield: 0.630 g (0.858 mmol, 86%). ^{1}H NMR (300 MHz, acetonitrile-d_3): δ (ppm) = 8.14 (*dd*, *J* = 9.0, 6.9 Hz, 1H), 8.07–8.01 (*m*, 2H), 7.99–7.94 (*m*, 3H), 7.75 (*qd*, *J* = 8.2 Hz, *J* = 1.2 Hz, 4H), 7.58 (*d*, *J* = 7.8 Hz, 2H), 4.22 (*s*, 6H), 2.51 (*s*, 6H). ^{13}C NMR (75 MHz, acetonitrile-d_3): δ (ppm) = 151.97, 135.33, 134.21, 133.95, 131.59, 129.21, 128.85, 127.87, 114.35, 113.82, 34.55, 18.20. ^{19}F NMR (235 MHz, acetonitrile-d_3): δ (ppm) = −79.31 (*s*, 6F). ATR-IR: $\tilde{\nu}$ (cm^{-1}) = 3066 (*w*), 3045 (*w*), 1604 (*w*), 1508 (*m*), 1498 (*m*), 1483 (*m*), 1463 (*m*), 1398 (*w*), 1319 (*w*), 1254 (*vs*), 1223 (*vs*), 1148 (*vs*), 1088 (*m*), 1028 (*vs*), 982 (*m*), 925 (*w*), 849 (*w*), 818 (*m*), 799 (*w*), 767 (*s*), 754 (*s*), 746 (*s*), 698 (*s*), 633 (*vs*), 573 (*s*), 559 (*s*), 515 (*vs*), 444 (*m*), 417 (*m*). ESI–MS: *m*/*z*(+) = calc. 581.10 [*M* + OTf]$^+$; found 581.10 [*M* + OTf]$^+$. *m*/*z*(−) = calc. 148.95 [OTf]$^-$; found 149.29 [OTf]$^-$.

2.3.4. Chalcogen-bonding donor 3^{Se}. A reported procedure was slightly modified for the synthesis of compound **3**^{Se} (Wonner *et al.*, 2017*a*, 2019*b*). To a flame-dried 50 ml Schlenk flask was added 0.150 g of **2**^{Se} (0.302 mmol, 1.00 eq.) dissolved in 20 ml dry DCM (15.1 m*M*). Afterwards, 85.5 µl methyl trifluoromethanesulfonate (0.124 g, 0.756 mmol, 2.50 eq.) was added dropwise. The mixture was stirred for 24 h at room temperature. The solvent was removed under reduced pressure. The crude solid was washed three times with diethyl ether and three times with pentane, and then dried under high vacuum. The crude solid was dissolved in the minimum amount of acetonitrile and precipitated by the addition of diethyl ether. The solid was filtered off and dried under high vacuum. Product **3**^{Se} was obtained as a pale-yellow solid (m.p. = 239 °C) after washing with diethyl ether and pentane. Yield: 0.230 g (0.278 mmol, 92%). ^{1}H NMR (400 MHz, acetonitrile-d_3): δ (ppm) = 8.14 (*dd*, *J* = 8.8, 6.7 Hz, 1H), 8.07–8.01 (*m*, 2H), 7.99–7.94 (*m*, 3H), 7.82–7.68 (*m*, 4H), 7.58 (*d*, *J* = 7.9 Hz, 2H), 4.22 (*s*, 6H), 2.50 (*s*, 6H). ^{13}C NMR (75 MHz, acetonitrile-d_3): δ (ppm) = 148.30, 136.11, 134.90, 134.21, 133.71, 128.93, 128.59, 128.28, 114.33, 113.87, 35.73, 11.10. ^{19}F NMR (377 MHz, chloroform-*d*): δ (ppm) = −79.34 (*s*, 6F). ATR-IR: $\tilde{\nu}$ (cm^{-1}) = 3082 (*w*), 2951 (*w*), 2360 (*w*), 1740 (*w*), 1605 (*w*), 1506 (*m*), 1476 (*m*), 1458 (*m*), 1404 (*w*), 1360 (*w*), 1308 (*w*), 1254 (*vs*), 1221 (*s*), 1138 (*s*), 1092 (*w*), 1078 (*w*), 1026 (*vs*), 935 (*w*), 908 (*w*), 829 (*w*), 773 (*w*), 758 (*s*), 739 (*m*), 710 (*w*), 692 (*m*), 667.37 (*w*), 633 (*vs*), 571 (*m*), 557 (*m*), 515 (*s*), 469 (*w*), 449 (*w*), 430 (*w*). ESI–MS: *m*/*z*(+) = calc. 676.99 [*M* − OTf]$^+$, 264.02 [*M* − 2OTf]$^{2+}$; found 676.64 [*M* − OTf]$^+$, 263.00 [*M* − 2OTf]$^{2+}$. *m*/*z*(−) = calc. 148.95 [OTf]$^-$; found 148.64 [OTf]$^-$.

2.4. Refinement

Crystal data, data collection and structure refinement details are summarized in Table 1. All H atoms were refined using the riding model in idealized positions and isotropic radii, with C—H distances of 0.98 Å and U_{iso}(H) = 1.5U_{eq}(C) for methyl H atoms, and C—H = 0.95 Å and U_{iso}(H) = 1.2U_{eq}(C) for other H atoms.

3. Discussion

As described in the *Introduction*, selenium-based chalcogen-bonding catalysts deriving from a 1,3-bis(benzimidazoliumyl) benzene frame were applied in several reactions. Whereas the first report describes the application in a stoichiometric activation of a carbon–bromine bond (Wonner *et al.*, 2017*a*), the following article dealt with the catalytic activation of a carbon–chloride bond (Wonner *et al.*, 2017*b*). As these reactions rely at least partially on the binding of the catalyst to the halide leaving group, they are typically easier to activate or catalyse than reactions involving neutral organic functional groups like carbonyls or imines. Therefore, the next step was the activation of quinolines in a transfer hydrogenation reaction (Wonner *et al.*, 2019*b*). However, this benchmark reaction showed surprisingly similar catalytic activities between preorganized and non-preorganized catalysts, as well as between sulfur- and selenium-based chalcogen-bonding donors. On theoretical grounds, the preorganized and the selenium-based variant would have been expected to be noticeably more potent. In particular, the comparable performance of the catalyst differing in the chalcogen atom was puzzling and intriguing, as this could mean that better accessible sulfur variants could be used in catalysis without much loss of turn-over frequency.

To further investigate this issue, the non-preorganized sulfur- and selenium-based catalysts were subjected to crystallization studies to investigate the chalcogen-bonding properties. Crystallization of these compounds proved difficult despite various efforts made while varying parameters that affect the crystallization process, such as temperature, concentration and crystallization techniques. The octyl chains, which are responsible for the good solubility of the catalysts in organic solvents, are most likely the reason for this. To avoid this challenge, the respective all-methylated catalysts (**3**^{S} and **3**^{Se}) were synthesized. The preparation of these compounds followed an already reported route (Fig. 1) (Wonner *et al.*, 2019*b*), with 1,3-bis(benzimidazolyl)benzene (Ganta & Chand, 2015) and compound **1** (Liu *et al.*, 2019) being synthesized according to literature procedures. The next step was the formation of the respective sulfur or selenium urea compounds (**2**^{S} and **2**^{Se}) under basic conditions. The final step, methylation of the urea compound, yielded the all-methylated compounds **3**^{S} and **3**^{Se}.

Next, crystallization studies were carried out. The vapour diffusion method was applied successfully to crystallize compound **3**^{S} from dichloromethane and cyclohexane (Fig. 2). This compound crystallizes in the monoclinic space group $P2_1/c$. The unit-cell constants are a = 7.7776 (2), b = 22.5823 (6) and c = 18.2338 (5) Å, with a volume of 3160.16 (15) Å^3 and a density of 1.536 Mg m^{-3}. The unit cell is built up of four ion pairs. Within this structure, an intermolecular interaction between atoms S1 and F1 of a trifluoromethanesulfonate anion is observed. The S1···F1 distance is 3.154 (3) Å, 96% of the van der Waals radii (Σr_ω), and the directionality is rather poor (C1—S1···F1 = 146.9°). The supposedly more Lewis basic O atoms of the trifluoromethanesulfonate anion are involved in two anion–π interactions with the imidazole unit of benzimidazole. These interactions have distances O6···cent = 2.894 (4) Å and O3···cent = 3.068 (3) Å from the calculated centroid (cent) of the imidazole unit to the trifluoromethanesulfonate O atoms. From this O atom to the closest C atom, the distances in both cases are 11% shorter than the Σr_ω (which possibly indicates a stronger interaction compared to the already mentioned chalcogen-bonding interaction). In addition, hydrogen bonding between atoms O4 and H15 in the 2-position of the central arene core [with H15···O4 = 2.468 (5) Å, 94% of Σr_ω, and C15—H15···O4 = 166.5°] is observed.

Overall, merely a chalcogen-bonding interaction between sulfur and fluorine was observed with a distance that corresponds to 96% of the Σr_ω. Additional weak hydrogen bonding found in this structure between the backbone H atoms of the arene core and the benzimidazolium unit will not be further discussed in this article.

Under the same crystallization conditions, the selenium-containing equivalent **3**^{Se} crystallizes also in the monoclinic space group $P2_1/c$ (Fig. 3). The unit-cell constants are a = 7.74775 (4), b = 13.12863 (8) and c = 31.27496 (18) Å, with a volume of 3181.02 (3) Å^3 and a density of 1.722 Mg m^{-3}. The unit cell contains four ion pairs and bidentate chalcogen bonding from the Se1 and Se2 centres of **3**^{Se} to trifluoromethanesulfonate atom O4 is observed. Some of the anions involved in these interactions are disordered over two positions. The interaction distances are Se1···O4 = 3.031 (2) Å and Se2···O4 = 3.080 (2) Å, with angles of C3—Se1···O4 = 165.31° and C11—Se2···O4 = 159.89°. The sum of the van der Waals radii is 3.42 Å and therefore the observed distances amount to 89 and 90% of this measure, thus classifying this interaction as stronger chalcogen bonding compared to the interaction found in the structure of **3**^{S}. Atom Se2, which already features chalcogen bonding in the elongation of the benzimidazole C11—Se bond, faces also a second chalcogen-bonding interaction to atom O3*A* of the second trifluoromethanesulfonate anion in the elongation of the CH_3—Se bond, with an Se2···O3*A* distance of 3.035 (3) Å and a C2—Se2···O3*A* angle of 158.07° (89% of Σr_ω). This additional interaction vividly demonstrates the property of chalcogens to form *two* noncovalent interactions based on their Lewis acidity. Although only one electron-withdrawing substituent is used, both axes simultaneously seem to be available for chalcogen bonding.

Taking a closer look at the unit cell, several other intermolecular interactions are found. The remaining O atoms (O5

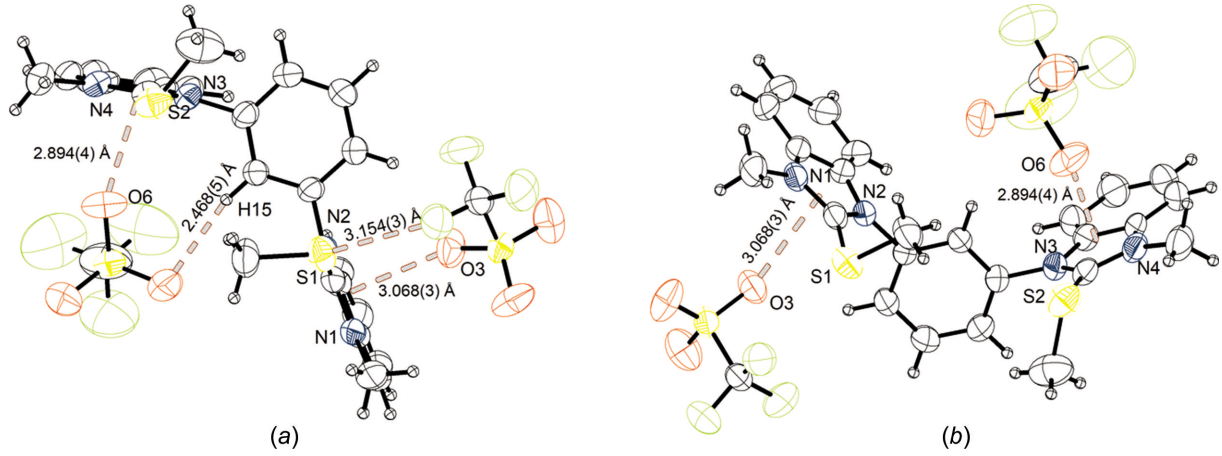

Figure 2
The molecular structure of **3**^{S} with the chalcogen bonding, anion–π interactions and hydrogen bonding marked, and with displacement ellipsoids drawn at the 50% probability level.

and O6) of this trifluoromethanesulfonate anion are involved in two anion–π interactions to an imidazole group of benzimidazole [O5···cent = 3.269 (3) Å and O6···cent = 3.307 (3) Å]. These interactions can be considered very weak, as the distances are close to the actual Σr_ω with 99 and 100%. Atom O5 faces additional hydrogen bonding, formed with atom H20 sitting in the 4-position of the central arene core [H20···O5 = 2.397 (2) Å, 91% of Σr_ω, and C20—H20···O5 = 143.01°]. Moreover, atom O1*A* of the trifluoromethanesulfonate anion is employed in a second hydrogen-bonding interaction to H24, sitting in the 2-position of the central arene core [H24···O1*A* = 2.402 (4) Å, 92% of Σr_ω, and C24—H24···O1*A* = 161.21°]. These two hydrogen-bonding interactions indicate a Lewis acidic character of the benzene H atoms. The overall picture of the unit cell is therefore described by two chalcogen-bonding donors which are bridged with two trifluoromethanesulfonate anions *via* chalcogen bonding, hydrogen bonding and anion–π interactions. This structure features comparable binding distances within the chalcogen-bonding donor, *e.g.* the distances of the carbon–selenium bonds and also similar distances of the observed intermolecular chalcogen bonding to a related compound (Wonner *et al.*, 2017*a*). The distances of the anion–π interactions in $\mathbf{3}^{\mathbf{S}}$ are on average 9% shorter than the corresponding interactions found in this crystal structure. This could be explained by the fact that one trifluoromethanesulfonate O atom forms this interaction in the structure of $\mathbf{3}^{\mathbf{S}}$, whereas two trifluoromethanesulfonate O atoms are involved in the interaction with $\mathbf{3}^{\mathbf{Se}}$, which geometrically leads to an increased interaction distance. Another explanation could be the more electron-withdrawing properties of sulfur compared to selenium based on the difference in their electronegativity, leading to a more polarized imidazolium system when sulfur is implemented.

Besides this structure, a second crystal structure (B) of $\mathbf{3}^{\mathbf{Se}}$ was obtained from crystallization at lower temperatures (4–5 °C) (Fig. 4). The crystal system is again monoclinic with the space group $P2_1/c$. The parameters of the unit cell are a = 13.8634 (4), b = 7.7558 (2) and c = 29.3267 (7) Å, with a volume of 3144.59 (14) Å^3 and a density of 1.742 Mg m^{-3}. The unit cell once more consists of four ion pairs. Different to the previously described solid-state structure (A of $\mathbf{3}^{\mathbf{Se}}$), each selenium centre features its own chalcogen-bonding interaction to an O atom of a trifluoromethanesulfonate anion. The distances of these interactions are Se1···O3 = 3.074 (4) Å (90% of Σr_ω) and Se2···O1 = 3.052 (4) Å (89% of Σr_ω), with C3—Se1···O3 = 167.87° and C5—Se2···O1 = 171.26°. Besides these interactions and differences, yet another short contact is observed. Atom Se1, already featuring chalcogen bonding in the elongation of the benzimidazole C3—Se1 bond, faces also a second chalcogen-bonding interaction to atom O5 of the second trifluoromethanesulfonate anion in the elongation of the CH_3—Se bond. This interaction [Se1···O5 = 3.033 (3) Å, 89% of Σr_ω, with C3—Se1···O5 = 161.19°] gives Se1 again a biaxial character. However, only one of the two Se atoms features this biaxial system, as also seen in structure A of $\mathbf{3}^{\mathbf{Se}}$ (Fig. 3). Between the two crystal structures of $\mathbf{3}^{\mathbf{Se}}$, only minor differences are observed, as the Se···O chalcogen-bonding interaction distances are in both cases approximately 90% of the van der Waals radii. The angles of the structure obtained at

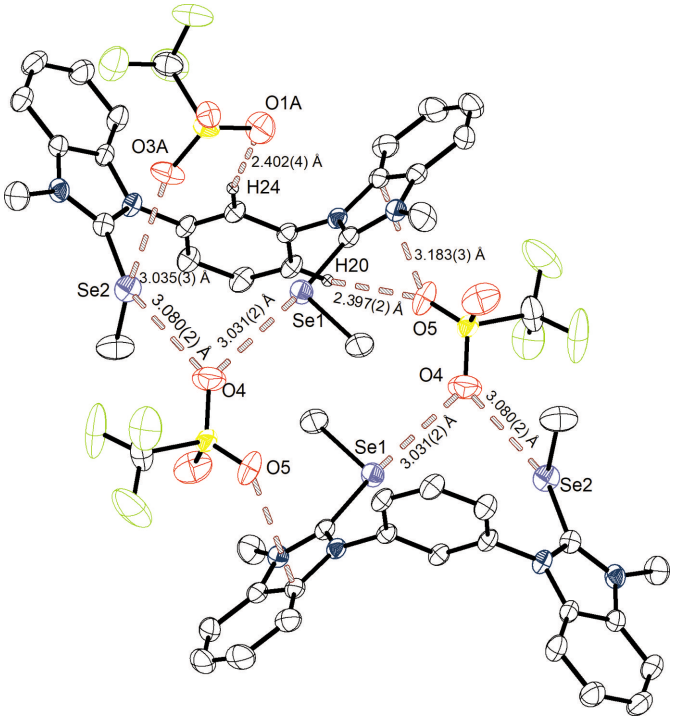

Figure 3
Structure A of $\mathbf{3}^{\mathbf{Se}}$ with the chalcogen bonding, hydrogen bonding and anion–π interactions marked, and with displacement ellipsoids drawn at the 50% probability level. For the sake of clarity, only H atoms involved in hydrogen bonding are shown. Symmetry operation to generate the second molecule of $\mathbf{3}^{\mathbf{Se}}$ and trifluoromethanesulfonate: $-x + 1$, $-y + 1$, $-x + 1$.

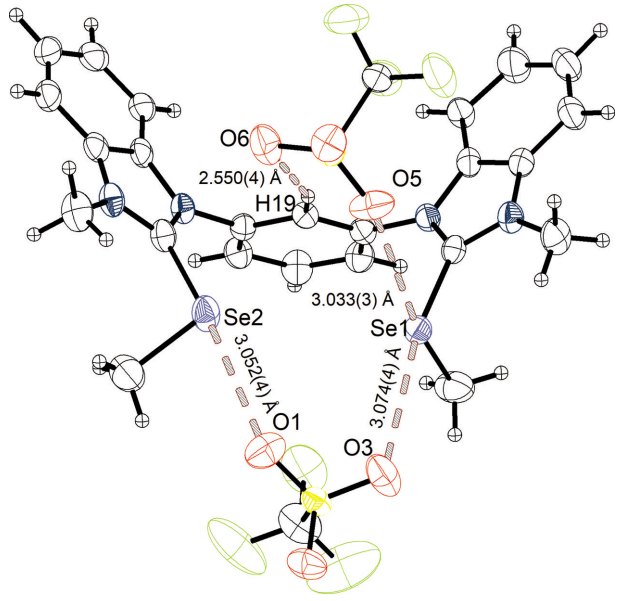

Figure 4
Structure B of $\mathbf{3}^{\mathbf{Se}}$ grown at 4–5 °C, with the chalcogen bonding and hydrogen bonding marked, and with displacement ellipsoids drawn at the 50% probability level.

lower temperatures are closer to 170°. Both structures feature a biaxial chalcogen centre with similar Se···O distances (89% of the van der Waals radii) and similar angles below 160°, which are less directional than the interactions in the elongation of the benzimidazole C—Se bond. Similar to the previously described structures, the 2-position hydrogen (H19) of the central arene core shows its Lewis acidic potential in a hydrogen-bonding interaction to one of the trifluoromethanesulfonate anions (O6) [H19···O6 = 2.550 (4) Å, 98% of Σr_ω, and C19—H19···O6 = 157.75°].

Changing the solvent in the crystallization experiments from dichloromethane to 1,2-dichloroethane ended up yielding yet another structural variation (structure C of $\mathbf{3}^{\mathbf{Se}}$) (Fig. 5). In this case, a triclinic space group $P\overline{1}$, with unit-cell parameters of a = 9.3672 (1), b = 13.3265 (2) and c = 13.6445 (1) Å, with a volume of 1647.49 (3) Å^3 and a density of 1.762 Mg m^{-3} was obtained. The unit cell is built up of two ion pairs along with four crystallized 1,2-dichloromethane molecules. The binding distances and angles within the donor are comparable to the previously described structure of $\mathbf{3}^{\mathbf{Se}}$. The crystal structure features two independent intermolecular interactions. The first one includes the Se1 centre and atom Cl1 of 1,2-dichloroethane, with an Se1···Cl1 distance of 3.535 (24) Å, which corresponds to 97% of the Σr_ω, and a C3*A*—Se1*A*···Cl1*A* angle of 176°. The second short contact can be found between the Se2 centre and trifluoromethanesulfonate atom O3, with an Se2···O3 distance of 3.133 (4) Å (92% of Σr_ω) and a C11—Se2···O3 angle of 168°. This Se···O interaction is again comparable to the other observed chalcogen-bonding interactions for $\mathbf{3}^{\mathbf{Se}}$. The distance of Se1*A* to the Cl1*A* atom of 1,2-dichloroethane is very close to the Σr_ω, which indicates a weaker interaction compared to the interaction of selenium with a trifluoromethanesulfonate O atom. However, since the solvent is not charged and thus a neutral chalcogen-bonding acceptor is involved in the Se···Cl interaction, a weaker interaction is expected. The slightly longer distance to the trifluoromethanesulfonate O atom compared to the distance in structures A and B of $\mathbf{3}^{\mathbf{Se}}$ can be explained by the fact that two independent Se···O/Cl chalcogen-bonding interactions, yet no co-operative effect, are present.

In addition, this structure also features anion–π interactions (Fig. 6). An imidazole moiety of one of the two benzimidazolium systems coordinates with each side to one trifluoromethanesulfonate anion [O1···cent = 3.152 (3) Å and O4*B*···cent = 3.063 (4) Å]. Atom O2 sitting on the same trifluoromethanesulfonate anion as O1 also forms an anion–π interaction [O2···cent = 2.920 (3) Å], becoming therefore a bridging moiety between two chalcogen-bonding donors. The imidazole system of this interaction does not feature a second anion–π interaction. The distances of these interactions are 5–13% shorter than the Σr_ω of the O atom to the closest C atom. These anion–π interactions are up to 10% shorter compared to those found in structure A of $\mathbf{3}^{\mathbf{Se}}$ (Fig. 4), and provide further indications that the weak anion–π interaction in structure A is due to geometric limitations. Comparing the interaction with $\mathbf{3}^{\mathbf{S}}$ indicates interactions of similar strength, even though selenium is less electronegative and does not polarize the imidazole moiety of benzimidazole in the same fashion as the more electronegative sulfur could do.

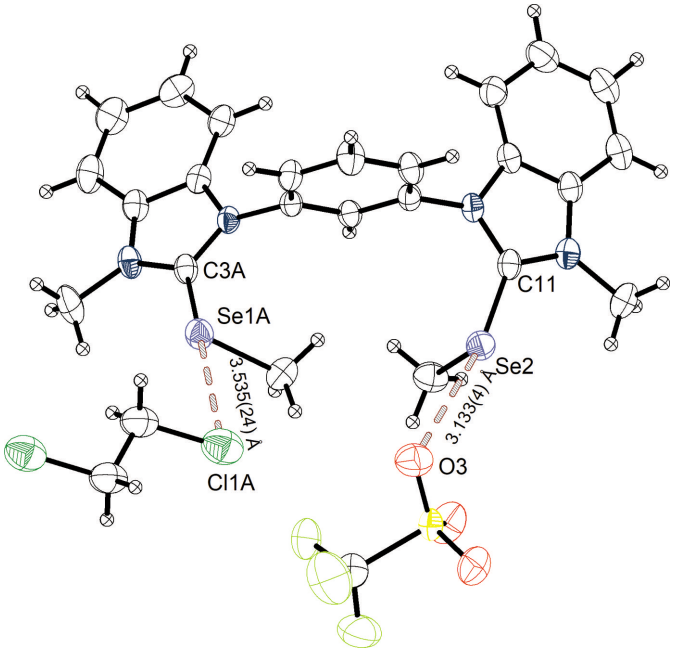

Figure 5
Structure C of $\mathbf{3}^{\mathbf{Se}}$, with chalcogen bonding to trifluoromethanesulfonate and 1,2-dichloroethane marked, and with displacement ellipsoids drawn at the 50% probability level. The dichloroethane molecule and trifluoromethanesulfonate anion are generated by (x + 1, y, z).

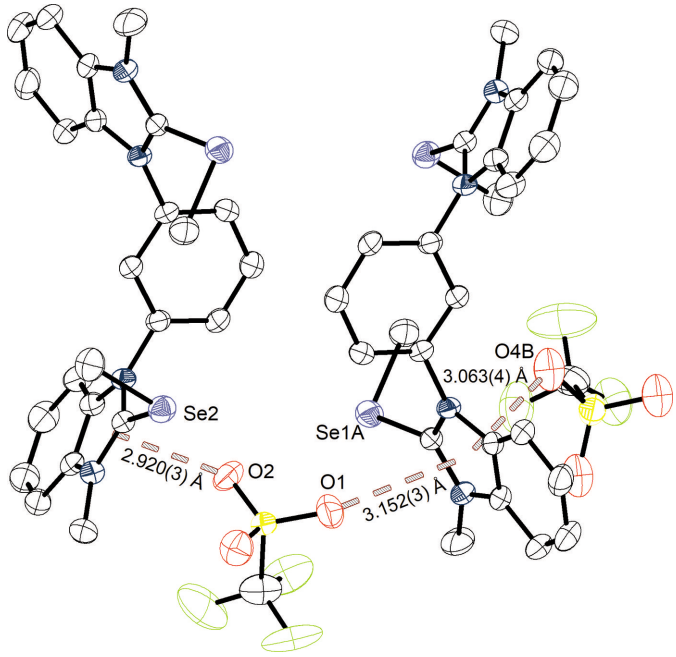

Figure 6
Structure C of $\mathbf{3}^{\mathbf{Se}}$, with the anion–π interactions to trifluoromethanesulfonate marked, and with displacement ellipsoids drawn at the 50% probability level. H atoms and 1,2-dichloroethane molecules have been omitted for clarity. The first trifluoromethanesulfonate anion is generated by (x, y, z − 1) and the second trifluoromethanesulfonate anion and $\mathbf{3}^{\mathbf{Se}}$ are generated by (−x + 1, −y + 1, −z).

Considering the fact that the carbon–nitrogen bonds to the central scaffold are free to rotate and therefore the Lewis acidic selenium centres could in principle point in opposite directions, it is interesting to see that a *syn*-like conformer has been observed in all of the presented structures. The only exception is the disorder found in structure C of **3**^{Se}, with a ratio of 95:5 of the *syn*- and *anti*-like conformers. This is especially remarkable for the structure of **3**^{S} and structure C of **3**^{Se}, as no bidentate interaction of the Lewis acidic centres keeps the compound in this conformation, and the last structure of **3**^{Se}, as two independent chalcogen-bonding interactions are found, which in principle could also point in different directions.

Overlaying the structure of **3**^{S} and structure B of **3**^{Se} stresses the similarity of the compounds (Fig. 7). The 1,3-bis-benzimidazolium scaffolds are matching each other in terms of geometry. The biggest difference is that one of the methyl groups located at the chalcogens (right side in this plot) is pointing in opposite direction. Nevertheless, they are roughly occupying the same space. The bigger difference is the orientation of one of the two trifluoromethanesulfonate anions. Whereas for **3**^{S}, the CF_3 group of trifluoromethanesulfonate is facing the sulfur, it is the SO_3 moiety that is facing the selenium centre in structure B of **3**^{Se}.

Besides these solid-state structures, we also performed density functional theory (DFT) calculations to further evaluate and elucidate chalcogen-bonding properties of the herein considered catalyst system. For the *in silico* investigations, the M06-2X functional (Zhao & Truhlar, 2008) with the triple-zeta def2-TZVP basis set (Weigend & Ahlrichs, 2005) and Grimme's D3 dispersion correction was applied (Grimme *et al.*, 2010; Grimme, 2012). In the electrostatic plots, the energy potentials are set to 87.8 and 153.1 kcal mol^{-1} and are projected with 0.001 e Bohr^{-3}. The surface map values are summed up in Table 2 in kcal mol^{-1}.

First, we consider the 'depth' of the σ-holes, which are localized at the elongation of the benzimidazole C—Ch bonds [Figs. 8(*a*), 8(*c*) and 8(*e*)]. According to the expected tendency, the surface map values for these σ-holes (at Ch1 and Ch2) are decreasing with the decreasing atomic number of the implemented chalcogen (Table 2). In any case, both σ-holes in the described areas show slightly different values (*e.g.* 152.4 and 153.3 kcal mol^{-1} for **3**^{Te}). The comparison of **3**^{Se} and **3**^{S} is of special interest, as these data can be compared with the previously reported catalysis data (Wonner *et al.*, 2019*b*). If a deeper σ-hole depth is equal to stronger catalytic activity, **3**^{Se} should show an increased activation compared to **3**^{S}. As stated above, this is not the case. Therefore, the observed catalytic activity in the reduction of quinolines cannot be further explained taking only these σ-holes into account.

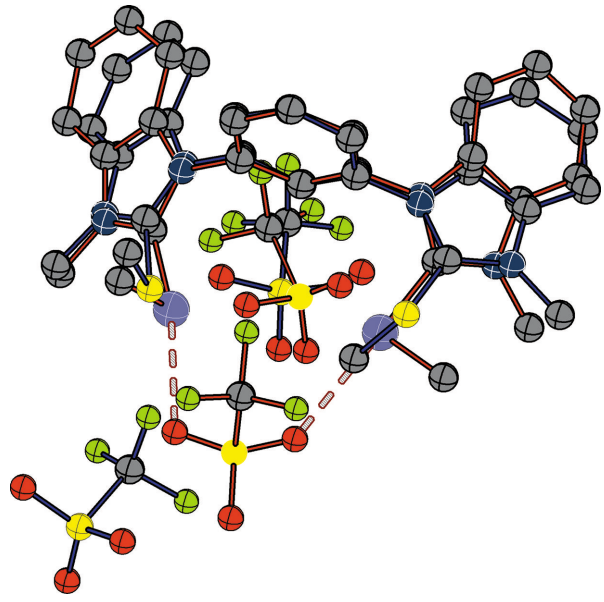

Figure 7
Overlay plot of the structures of **3**^{S} (blue bonds) and **3**^{Se} (structure B) (red bonds).

Shining light on the remaining σ-holes of these systems, that in the elongation of the CH_3—Ch bond [Figs. 8(*b*), 8(*d*) and 8(*f*)] could provide hints on the origins of the comparable catalytic properties. **3**^{Te} shows defined σ-holes [Fig. 8(*b*)] in this region with decreased absolute values of potentials [with respect to those of the C(benzim)—Ch bond] of 147.8 and 147.2 kcal mol^{-1}. Besides this electron-poor area, the H atom in the 2-position of the central arene core also features an electropositive potential of 145.2 kcal mol^{-1}.

Moving to **3**^{Se}, these σ-holes are less defined and less separated from the electron-poor region at the central arene core [Fig. 8(*d*)]. In contrast to **3**^{Te}, the four chalcogen-based electron-deficient areas for **3**^{Se} show comparable energies (Table 2, entry 2). The estimated energy for the σ-hole of the 2-position H atom shows a potentially more Lewis acidic area compared to those located at the chalcogen. In two of the three crystal structures of **3**^{Se}, we observed weak hydrogen bonding of this H atom. The overall maximum value for **3**^{Se} was observed right between the less defined chalcogen and hydrogen σ-hole, with a value of 147.9 kcal mol^{-1}. For **3**^{Te}, no such value was found, as they did not overcome the classic σ-hole values.

Continuing these investigations with **3**^{S}, no separation of the σ-holes (CH_3—S bond) is spotted and a connected electron-

Table 2
Surface map values for the σ-holes of **3**^{Ch}.

Entry	Compound	C(benzim)—Ch1[a]	C(benzim)—Ch2[a]	CH_3—Ch1[a]	CH_3—Ch2[a]	C(core)—H[b]	Maximum
1	**3**^{Te}	152.4	153.3	147.8	147.2	145.2	–
2	**3**^{Se}	146.6	144.7	145.9	145.6	146.9[c]	147.9
3	**3**^{S}	141.0	144.2	144.5	144.9[c]	146.6[c]	149.1

Notes: (*a*) surface map values in kcal mol^{-1} in the elongation of the respective bonds, (*b*) the H atom at the 2-position of the central benzene core and (*c*) approximate values due to the unclear definition of the σ-holes.

deficient system covering these σ-holes and the 2-position H atom of the central core is observed. The surface map values (Table 2, entry 3) are reversed to those from $\mathbf{3}^{\mathbf{Te}}$, as the 2-position seems to be the most Lewis acidic centre, followed by the CH_3—S bond σ-holes. The C(benzim)—S bond σ-holes are those that are the least Lewis acidic. Matching this with the crystal structure of $\mathbf{3}^{\mathbf{S}}$, these data are confirmed, as no chalcogen bonding in the elongation of the C(benzim)—S bond is found, but one intermolecular action is observed in the elongation of the CH_3—S bond which is theoretically favoured. Like $\mathbf{3}^{\mathbf{Se}}$, the most electron-deficient area of $\mathbf{3}^{\mathbf{S}}$ is again observed between the central arene core and the chalcogen. However, in the case of $\mathbf{3}^{\mathbf{S}}$, the difference to the second most Lewis acidic centre (2.5 kcal mol^{-1}) is larger than the difference in $\mathbf{3}^{\mathbf{Se}}$ (1.0 kcal mol^{-1}). Since sulfur is more electron withdrawing, the larger electron deficient area might be explained by the more electron-withdrawing sulfur, which impacts the whole structure. This might also explain the reason for the catalytic activity in the reduction of quinolones. Nevertheless, it is necessary to mention that various reference experiments were carried out in that reaction which indicate an activation based on chalcogen bonding, for instance, by using the respective hydrogen-bonding equivalents.

4. Conclusion

In summary, we presented four solid-state structures of sulfur- and selenium-containing chalcogen-bonding catalysts. The

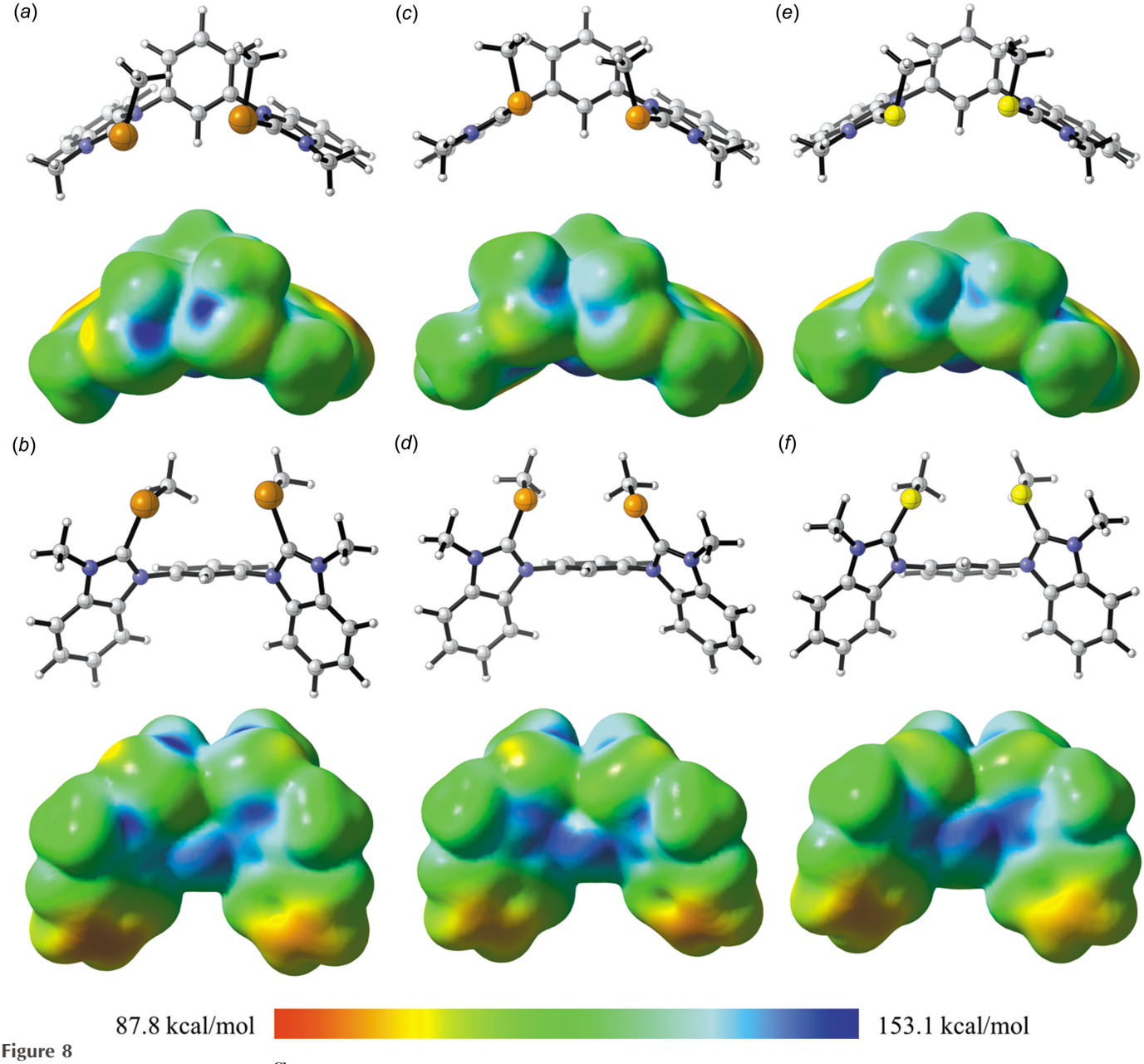

Figure 8
Plots of the optimized structure of $\mathbf{3}^{\mathbf{Ch}}$ created with *CLYView* (Legault, 2009), along with the electrostatic potential surface with an energy scale of 87.8–153.1 kcal mol^{-1} projected with 0.001 e Bohr^{-3}. (*a*)/(*b*) Ch = Te, (*c*)/(*d*) Ch = Se and (*e*)/(*f*) Ch = S.

structures and their interactions are matched with *in silico*-calculated respective structures to shine some light on the fairly surprising results of their application in the activation of quinolines. The structure of $\mathbf{3}^{\mathbf{S}}$ features one chalcogen-bonding interaction from sulfur to fluorine of the trifluoromethanesulfonate counter-anion, which has an interaction distance close to the sum of the van der Waals radii, whilst also anion–π interactions and hydrogen bonding are observed. These results are in line with the theoretically predicted data. In three crystal structures of the selenium-based analogue $\mathbf{3}^{\mathbf{Se}}$, different mono- and bidentate, as well as biaxial binding motifs to neutral and negatively charged molecules based on chalcogen bonding, are present. Nevertheless, these structures also contained anion–π interactions along with hydrogen bonding. The results could also be related to calculational data. We further extended the DFT calculations to the appropriate tellurium-based compound, which could not be synthesized, and observed the most suitable theoretical properties for chalcogen bonding. However, the unusual activities of the previous report on the reduction of quinolines could not be satisfactorily explained.

Acknowledgements

Funding by the Deutsche Forschungsgemeinschaft (DFG, Germany Research Foundation) under Germany's Excellence Strategy is gratefully acknowledged. The authors declare no conflict of interest. Open access funding enabled and organized by Projekt DEAL.

Funding information

The following funding is acknowledged: Deutsche Forschungsgemeinschaft (grant Nos. EXC 2033-390677874-RESOLV and HU1782/5-1).

References

Aakeroy, C. B., Bryce, D. L., Desiraju, G. R., Frontera, A., Legon, A. C., Nicotra, F., Rissanen, K., Scheiner, S., Terraneo, G., Metrangolo, P. & Resnati, G. (2019). *Pure Appl. Chem.* **91**, 1889–1892.
Benz, S., López–Andarias, J., Mareda, J., Sakai, N. & Matile, S. (2017). *Angew. Chem. Int. Ed.* **56**, 812–815.
Benz, S., Macchione, M., Verolet, Q., Mareda, J., Sakai, N. & Matile, S. (2016). *J. Am. Chem. Soc.* **138**, 9093–9096.
Bleiholder, C., Werz, D. B., Köppel, H. & Gleiter, R. (2006). *J. Am. Chem. Soc.* **128**, 2666–2674.
Cavallo, G., Metrangolo, P., Milani, R., Pilati, T., Priimagi, A., Resnati, G. & Terraneo, G. (2016). *Chem. Rev.* **116**, 2478–2601.
Doyle, A. G. & Jacobsen, E. N. (2007). *Chem. Rev.* **107**, 5713–5743.
Dupont, L., Dideberg, O. & Jacquemin, P. (1990). *Acta Cryst.* C**46**, 484–486.
Farrugia, L. J. (2012). *J. Appl. Cryst.* **45**, 849–854.
Fujita, K., Iwaoka, M. & Tomoda, S. (1994). *Chem. Lett.* **23**, 923–926.
Ganta, S. & Chand, D. K. (2015). *Dalton Trans.* **44**, 15181–15188.
Garrett, G. E., Gibson, G. L., Straus, R. N., Seferos, D. S. & Taylor, M. S. (2015). *J. Am. Chem. Soc.* **137**, 4126–4133.
Grimme, S. (2012). *Chem. Eur. J.* **18**, 9955–9964.
Grimme, S., Antony, J., Ehrlich, S. & Krieg, H. (2010). *J. Chem. Phys.* **132**, 154104.
Hübschle, C. B., Sheldrick, G. M. & Dittrich, B. (2011). *J. Appl. Cryst.* **44**, 1281–1284.
Jungbauer, S. H. & Huber, S. M. (2015). *J. Am. Chem. Soc.* **137**, 12110–12120.
Kubiniok, S., du Mont, W.-W., Pohl, S. & Saak, W. (1988). *Angew. Chem. Int. Ed. Engl.* **27**, 431–433.
Legault, C. Y. (2009). *CYLview*. Version 1.0b. Université de Sherbrooke, Canada.
Liu, X., Ma, S. & Toy, P. H. (2019). *Org. Lett.* **21**, 9212–9216.
Macchione, M., Tsemperouli, M., Goujon, A., Mallia, A. R., Sakai, N., Sugihara, K. & Matile, S. (2018). *Helv. Chim. Acta*, **101**, e1800014.
Macrae, C. F., Sovago, I., Cottrell, S. J., Galek, P. T. A., McCabe, P., Pidcock, E., Platings, M., Shields, G. P., Stevens, J. S., Towler, M. & Wood, P. A. (2020). *J. Appl. Cryst.* **53**, 226–235.
Mulliken, R. S. (1952). *J. Am. Chem. Soc.* **74**, 811–824.
Putz, H. & Brandenburg, K. (2014). *DIAMOND*. Crystal Impact GbR, Bonn, Germany. https://www.crystalimpact.de/diamond.
Rigaku OD (2018). *CrysAlis PRO*. Rigaku Oxford Diffraction Ltd, Yarnton, Oxfordshire, England.
Rosenfield, R. E., Parthasarathy, R. & Dunitz, J. D. (1977). *J. Am. Chem. Soc.* **99**, 4860–4862.
Sheldrick, G. M. (2015*a*). *Acta Cryst.* A**71**, 3–8.
Sheldrick, G. M. (2015*b*). *Acta Cryst.* C**71**, 3–8.
Steinke, T., Wonner, P., Engelage, E. & Huber, S. M. (2021). *Synthesis*, **53**, 2043–2050.
Steinke, T., Wonner, P., Gauld, R. M., Heinrich, S. & Huber, S. M. (2022). *Chem. A Eur. J.* **28**, e202200917.
Tiecco, M., Testaferri, L., Santi, C., Tomassini, C., Marini, F., Bagnoli, L. & Temperini, A. (2002). *Chem. Eur. J.* **8**, 1118–1124.
Wang, W., Zhu, H., Liu, S., Zhao, Z., Zhang, L., Hao, J. & Wang, Y. (2019). *J. Am. Chem. Soc.* **141**, 9175–9179.
Weigend, F. & Ahlrichs, R. (2005). *Phys. Chem. Chem. Phys.* **7**, 3297–3305.
Weiss, R., Aubert, E., Pale, P. & Mamane, V. (2021). *Angew. Chem. Int. Ed.* **60**, 19281–19286.
Werz, D. B., Gleiter, R. & Rominger, F. (2002). *J. Am. Chem. Soc.* **124**, 10638–10639.
Werz, D. B., Gleiter, R. & Rominger, F. (2004). *J. Org. Chem.* **69**, 2945–2952.
Wirth, T. (1995). *Angew. Chem. Int. Ed. Engl.* **34**, 1726–1728.
Wonner, P., Dreger, A., Vogel, L., Engelage, E. & Huber, S. M. (2019*a*). *Angew. Chem. Int. Ed.* **58**, 16923–16927.
Wonner, P., Steinke, T. & Huber, S. M. (2019*b*). *Synlett*, **30**, 1673–1678.
Wonner, P., Steinke, T., Vogel, L. & Huber, S. M. (2020). *Chem. Eur. J.* **26**, 1258–1262.
Wonner, P., Vogel, L., Düser, M., Gomes, L., Kniep, F., Mallick, B., Werz, D. B. & Huber, S. M. (2017*a*). *Angew. Chem. Int. Ed.* **56**, 12009–12012.
Wonner, P., Vogel, L., Kniep, F. & Huber, S. M. (2017*b*). *Chem. Eur. J.* **23**, 16972–16975.
Zhao, H. & Gabbaï, F. P. (2010). *Nat. Chem.* **2**, 984–990.
Zhao, Y. & Truhlar, D. G. (2008). *Theor. Chem. Acc.* **120**, 215–241.
Zhou, B. & Gabbaï, F. P. (2021). *J. Am. Chem. Soc.* **143**, 8625–8630.

supporting information

Acta Cryst. (2023). C**79**, 26-35 [https://doi.org/10.1107/S2053229622011536]

Chalcogen bonding in the solid-state structures of 1,3-bis-(benzimidazoliumyl)benzene-based chalcogen-bonding donors

Tim Steinke, Elric Engelage and Stefan M. Huber

Computing details

For all structures, data collection: *CrysAlis PRO* (Rigaku OD, 2018); cell refinement: *CrysAlis PRO* (Rigaku OD, 2018); data reduction: *CrysAlis PRO* (Rigaku OD, 2018); program(s) used to solve structure: SHELXT (Sheldrick, 2015a) and shelXle (Hübschle *et al.*, 2011); program(s) used to refine structure: *SHELXL2018* (Sheldrick, 2015b); molecular graphics: *DIAMOND* (Putz & Brandenburg, 2014) and *Mercury* (Macrae *et al.*, 2020); software used to prepare material for publication: *WinGX* (Farrugia, 2012).

3,3′-Bis(methylsulfanyl)-1,1′-(1,3-phenylene)bis(1*H*-1,3-benzodiazol-3-ium) bis(trifluoromethanesulfonate) (ts-049_3S)

Crystal data

$C_{24}H_{24}N_4S_2^{2+}\cdot 2CF_3O_3S^-$
M_r = 730.73
Monoclinic, $P2_1/c$
a = 7.7776 (2) Å
b = 22.5823 (6) Å
c = 18.2338 (5) Å
β = 99.329 (2)°
V = 3160.16 (15) Å^3
Z = 4
$F(000)$ = 1496
D_x = 1.536 Mg m^{-3}
Cu $K\alpha$ radiation, λ = 1.54184 Å
Cell parameters from 5564 reflections
θ = 3.1–66.5°
μ = 3.51 mm^{-1}
T = 170 K
Needle, translucent white
0.13 × 0.06 × 0.03 mm

Data collection

Rigaku XtaLAB Synergy Dualflex diffractometer with a HyPix detector
Radiation source: micro-focus sealed X-ray tube, PhotonJet (Cu) X-ray Source
Mirror monochromator
ω scans
Absorption correction: multi-scan (CrysAlis PRO; Rigaku OD, 2018)
T_{min} = 0.579, T_{max} = 1.000
21606 measured reflections
5564 independent reflections
4631 reflections with $I > 2\sigma(I)$
R_{int} = 0.043
θ_{max} = 66.5°, θ_{min} = 3.1°
h = −9→5
k = −25→26
l = −21→21

Refinement

Refinement on F^2
Least-squares matrix: full
$R[F^2 > 2\sigma(F^2)]$ = 0.073
$wR(F^2)$ = 0.205
S = 1.09
5564 reflections
419 parameters
0 restraints
Hydrogen site location: inferred from neighbouring sites
H-atom parameters constrained

$w = 1/[\sigma^2(F_o^2) + (0.0868P)^2 + 6.2578P]$
where $P = (F_o^2 + 2F_c^2)/3$
$(\Delta/\sigma)_{max} < 0.001$

$\Delta\rho_{max} = 0.69$ e Å^{-3}
$\Delta\rho_{min} = -0.39$ e Å^{-3}

Special details

Geometry. All e.s.d.'s (except the e.s.d. in the dihedral angle between two l.s. planes) are estimated using the full covariance matrix. The cell e.s.d.'s are taken into account individually in the estimation of e.s.d.'s in distances, angles and torsion angles; correlations between e.s.d.'s in cell parameters are only used when they are defined by crystal symmetry. An approximate (isotropic) treatment of cell e.s.d.'s is used for estimating e.s.d.'s involving l.s. planes.

Fractional atomic coordinates and isotropic or equivalent isotropic displacement parameters (Å^2)

	x	*y*	*z*	U_{iso}*/U_{eq}
S1	0.35126 (16)	0.56835 (6)	0.25113 (7)	0.0608 (4)
N1	0.3348 (5)	0.50402 (16)	0.3780 (2)	0.0540 (10)
O1	−0.0399 (6)	0.41389 (17)	0.2140 (3)	0.0872 (13)
F1	0.0689 (4)	0.51149 (15)	0.12752 (18)	0.0726 (8)
C1	0.5501 (7)	0.6107 (3)	0.2717 (3)	0.0715 (15)
H1A	0.579226	0.627305	0.225622	0.107*
H1AB	0.644929	0.584853	0.294772	0.107*
H1AC	0.534172	0.642930	0.305987	0.107*
C2	0.3914 (7)	0.4486 (2)	0.3489 (4)	0.0719 (16)
H2A	0.289278	0.425239	0.327712	0.108*
H2AB	0.461306	0.426270	0.389191	0.108*
H2AC	0.461914	0.457087	0.310199	0.108*
S2	0.49729 (19)	0.80031 (6)	0.25935 (8)	0.0670 (4)
N2	0.2444 (4)	0.59565 (15)	0.3825 (2)	0.0443 (8)
O2	−0.2997 (5)	0.4683 (2)	0.2232 (3)	0.0866 (13)
F2	−0.1862 (5)	0.48431 (17)	0.0786 (2)	0.0926 (11)
S3	−0.11679 (15)	0.47000 (5)	0.22368 (7)	0.0541 (3)
N3	0.3109 (5)	0.80886 (15)	0.3752 (2)	0.0470 (9)
O3	−0.0234 (5)	0.50764 (17)	0.2798 (2)	0.0698 (10)
F3	−0.1486 (5)	0.56541 (14)	0.1402 (2)	0.0952 (12)
C3	0.3109 (5)	0.55545 (19)	0.3401 (3)	0.0494 (11)
C4	0.2803 (5)	0.5108 (2)	0.4456 (3)	0.0520 (11)
S4	0.77237 (17)	0.72091 (5)	0.48588 (8)	0.0614 (4)
N4	0.5248 (5)	0.87227 (16)	0.3815 (2)	0.0536 (10)
O4	0.6806 (7)	0.66722 (19)	0.4697 (4)	0.118 (2)
F4	0.7760 (9)	0.7011 (3)	0.6268 (3)	0.157 (2)
C5	0.2729 (7)	0.4715 (2)	0.5046 (4)	0.0674 (16)
H5	0.310860	0.431642	0.503126	0.081*
O5	0.9570 (5)	0.71609 (19)	0.5008 (3)	0.0824 (12)
F5	0.5543 (10)	0.7495 (4)	0.5733 (4)	0.197 (4)
O6	0.7038 (6)	0.76858 (18)	0.4399 (3)	0.0870 (13)
F6	0.8004 (12)	0.7926 (3)	0.5986 (3)	0.183 (3)
C6	0.2087 (7)	0.4934 (3)	0.5638 (3)	0.0711 (16)
H6	0.200375	0.467634	0.604257	0.085*
C7	0.1544 (7)	0.5519 (3)	0.5683 (3)	0.0658 (14)
H7	0.112974	0.565088	0.611725	0.079*

C8	0.1598 (6)	0.5913 (2)	0.5103 (3)	0.0560 (12)
H8	0.120478	0.631015	0.511917	0.067*
C9	0.2250 (5)	0.56933 (19)	0.4506 (3)	0.0470 (10)
C25	−0.0943 (6)	0.5092 (2)	0.1387 (3)	0.0575 (12)
C10	0.1780 (5)	0.65309 (18)	0.3587 (2)	0.0427 (9)
C13	0.0411 (6)	0.7624 (2)	0.3156 (3)	0.0540 (11)
H13	−0.005869	0.800385	0.301595	0.065*
C12	−0.0553 (7)	0.7121 (2)	0.2967 (3)	0.0618 (13)
H12	−0.169567	0.715418	0.269176	0.074*
C11	0.0119 (6)	0.6568 (2)	0.3173 (3)	0.0540 (11)
H11	−0.054144	0.622075	0.303404	0.065*
C15	0.2777 (5)	0.70264 (18)	0.3781 (2)	0.0431 (9)
H15	0.391374	0.699598	0.406269	0.052*
C14	0.2070 (6)	0.75701 (18)	0.3553 (2)	0.0451 (10)
C16	0.3153 (6)	0.84064 (18)	0.4413 (3)	0.0481 (10)
C17	0.2144 (7)	0.8362 (2)	0.4963 (3)	0.0597 (13)
H17	0.120517	0.808961	0.493525	0.072*
C18	0.2588 (8)	0.8743 (2)	0.5563 (3)	0.0683 (14)
H18	0.194119	0.873057	0.596247	0.082*
C19	0.3968 (9)	0.9144 (2)	0.5590 (3)	0.0742 (17)
H19	0.421558	0.940111	0.600630	0.089*
C26	0.7166 (13)	0.7413 (5)	0.5744 (5)	0.111 (3)
C20	0.4967 (7)	0.9181 (2)	0.5047 (3)	0.0645 (14)
H20	0.591175	0.945075	0.507464	0.077*
C21	0.4523 (6)	0.87969 (17)	0.4445 (3)	0.0501 (11)
C22	0.6779 (7)	0.9045 (2)	0.3644 (4)	0.0718 (16)
H22A	0.706455	0.890325	0.317005	0.108*
H22B	0.777133	0.897555	0.403977	0.108*
H22C	0.652004	0.946926	0.360821	0.108*
C23	0.4388 (6)	0.82879 (18)	0.3403 (3)	0.0493 (10)
C24	0.3058 (10)	0.8150 (3)	0.1931 (4)	0.091 (2)
H24A	0.334857	0.813690	0.142782	0.137*
H24B	0.260693	0.854357	0.202400	0.137*
H24C	0.217090	0.785069	0.197802	0.137*

Atomic displacement parameters (Å²)

	U^{11}	U^{22}	U^{33}	U^{12}	U^{13}	U^{23}
S1	0.0561 (7)	0.0656 (8)	0.0585 (7)	−0.0077 (6)	0.0024 (5)	−0.0152 (6)
N1	0.044 (2)	0.0352 (19)	0.075 (3)	−0.0007 (15)	−0.0119 (19)	−0.0064 (18)
O1	0.117 (3)	0.044 (2)	0.107 (3)	0.011 (2)	0.038 (3)	0.012 (2)
F1	0.0648 (18)	0.076 (2)	0.076 (2)	−0.0092 (15)	0.0057 (15)	0.0123 (16)
C1	0.065 (3)	0.073 (4)	0.073 (4)	−0.024 (3)	0.000 (3)	−0.003 (3)
C2	0.065 (3)	0.040 (3)	0.105 (5)	0.008 (2)	−0.007 (3)	−0.011 (3)
S2	0.0748 (8)	0.0602 (8)	0.0694 (9)	0.0106 (6)	0.0218 (7)	0.0042 (6)
N2	0.0456 (19)	0.0336 (17)	0.050 (2)	−0.0044 (14)	−0.0049 (15)	−0.0005 (15)
O2	0.059 (2)	0.104 (3)	0.099 (3)	−0.018 (2)	0.017 (2)	−0.023 (3)
F2	0.104 (3)	0.090 (2)	0.071 (2)	−0.027 (2)	−0.0237 (19)	−0.0061 (18)

S3	0.0519 (6)	0.0430 (6)	0.0658 (7)	−0.0074 (5)	0.0044 (5)	−0.0067 (5)
N3	0.050 (2)	0.0331 (18)	0.056 (2)	−0.0003 (15)	0.0019 (17)	−0.0019 (16)
O3	0.075 (2)	0.068 (2)	0.061 (2)	−0.0241 (18)	−0.0018 (18)	−0.0094 (18)
F3	0.115 (3)	0.0526 (19)	0.110 (3)	0.0221 (18)	−0.008 (2)	0.0145 (18)
C3	0.039 (2)	0.038 (2)	0.066 (3)	−0.0016 (17)	−0.0071 (19)	−0.006 (2)
C4	0.039 (2)	0.041 (2)	0.069 (3)	−0.0034 (18)	−0.011 (2)	0.007 (2)
S4	0.0610 (7)	0.0418 (6)	0.0767 (9)	0.0067 (5)	−0.0030 (6)	0.0067 (6)
N4	0.050 (2)	0.0355 (19)	0.073 (3)	0.0002 (16)	0.0037 (19)	0.0095 (18)
O4	0.105 (4)	0.051 (2)	0.172 (5)	−0.009 (2)	−0.052 (3)	0.012 (3)
F4	0.177 (5)	0.190 (6)	0.107 (4)	0.019 (4)	0.028 (4)	0.063 (4)
C5	0.054 (3)	0.043 (3)	0.094 (4)	−0.004 (2)	−0.021 (3)	0.017 (3)
O5	0.061 (2)	0.077 (3)	0.107 (3)	0.0120 (19)	0.005 (2)	0.002 (2)
F5	0.156 (5)	0.274 (9)	0.188 (6)	0.080 (6)	0.110 (5)	0.087 (6)
O6	0.103 (3)	0.063 (2)	0.093 (3)	0.032 (2)	0.011 (2)	0.022 (2)
F6	0.297 (10)	0.146 (5)	0.104 (4)	0.022 (6)	0.022 (5)	−0.047 (4)
C6	0.067 (3)	0.070 (4)	0.069 (4)	−0.015 (3)	−0.011 (3)	0.030 (3)
C7	0.059 (3)	0.072 (4)	0.061 (3)	−0.009 (3)	−0.006 (2)	0.013 (3)
C8	0.053 (3)	0.056 (3)	0.054 (3)	−0.001 (2)	−0.004 (2)	0.009 (2)
C9	0.043 (2)	0.040 (2)	0.053 (3)	−0.0036 (18)	−0.0056 (19)	0.0060 (19)
C25	0.056 (3)	0.046 (3)	0.064 (3)	−0.001 (2)	−0.014 (2)	−0.006 (2)
C10	0.048 (2)	0.033 (2)	0.044 (2)	0.0002 (17)	−0.0016 (18)	−0.0010 (17)
C13	0.054 (3)	0.040 (2)	0.064 (3)	0.0059 (19)	−0.002 (2)	0.006 (2)
C12	0.052 (3)	0.052 (3)	0.072 (3)	0.000 (2)	−0.017 (2)	0.002 (2)
C11	0.049 (2)	0.042 (2)	0.065 (3)	−0.0054 (19)	−0.010 (2)	−0.002 (2)
C15	0.043 (2)	0.037 (2)	0.046 (2)	0.0008 (17)	−0.0032 (17)	−0.0030 (17)
C14	0.053 (2)	0.034 (2)	0.047 (2)	−0.0027 (18)	0.0026 (19)	−0.0025 (17)
C16	0.053 (2)	0.034 (2)	0.054 (3)	0.0054 (18)	0.001 (2)	−0.0024 (18)
C17	0.067 (3)	0.042 (3)	0.067 (3)	0.000 (2)	0.000 (2)	−0.010 (2)
C18	0.089 (4)	0.058 (3)	0.057 (3)	0.006 (3)	0.009 (3)	−0.009 (2)
C19	0.096 (4)	0.048 (3)	0.068 (4)	−0.002 (3)	−0.018 (3)	−0.013 (3)
C26	0.122 (7)	0.122 (7)	0.094 (6)	0.036 (5)	0.034 (5)	0.042 (5)
C20	0.069 (3)	0.039 (3)	0.076 (4)	−0.004 (2)	−0.015 (3)	−0.003 (2)
C21	0.056 (3)	0.025 (2)	0.062 (3)	0.0002 (17)	−0.011 (2)	0.0046 (18)
C22	0.058 (3)	0.053 (3)	0.103 (5)	−0.012 (2)	0.008 (3)	0.016 (3)
C23	0.053 (2)	0.034 (2)	0.060 (3)	0.0040 (18)	0.002 (2)	0.0091 (19)
C24	0.112 (5)	0.101 (5)	0.059 (3)	0.032 (4)	0.008 (3)	0.002 (3)

Geometric parameters (Å, º)

S1—C3	1.726 (5)	C5—C6	1.353 (9)
S1—C1	1.806 (5)	C5—H5	0.9500
N1—C3	1.350 (6)	F5—C26	1.273 (10)
N1—C4	1.375 (7)	F6—C26	1.367 (12)
N1—C2	1.455 (6)	C6—C7	1.394 (8)
O1—S3	1.424 (4)	C6—H6	0.9500
F1—C25	1.319 (6)	C7—C8	1.387 (7)
C1—H1A	0.9800	C7—H7	0.9500
C1—H1AB	0.9800	C8—C9	1.365 (7)

C1—H1AC	0.9800	C8—H8	0.9500
C2—H2A	0.9800	C10—C15	1.375 (6)
C2—H2AB	0.9800	C10—C11	1.388 (6)
C2—H2AC	0.9800	C13—C12	1.374 (7)
S2—C23	1.737 (5)	C13—C14	1.379 (6)
S2—C24	1.790 (7)	C13—H13	0.9500
N2—C3	1.349 (6)	C12—C11	1.382 (7)
N2—C9	1.407 (6)	C12—H12	0.9500
N2—C10	1.437 (5)	C11—H11	0.9500
O2—S3	1.422 (4)	C15—C14	1.382 (6)
F2—C25	1.332 (5)	C15—H15	0.9500
S3—O3	1.434 (4)	C16—C17	1.373 (7)
S3—C25	1.818 (6)	C16—C21	1.377 (6)
N3—C23	1.342 (6)	C17—C18	1.390 (7)
N3—C16	1.400 (6)	C17—H17	0.9500
N3—C14	1.435 (5)	C18—C19	1.399 (9)
F3—C25	1.339 (6)	C18—H18	0.9500
C4—C9	1.397 (6)	C19—C20	1.357 (9)
C4—C5	1.403 (7)	C19—H19	0.9500
S4—O4	1.414 (4)	C20—C21	1.398 (7)
S4—O6	1.415 (4)	C20—H20	0.9500
S4—O5	1.422 (4)	C22—H22A	0.9800
S4—C26	1.797 (9)	C22—H22B	0.9800
N4—C23	1.347 (6)	C22—H22C	0.9800
N4—C21	1.369 (7)	C24—H24A	0.9800
N4—C22	1.471 (6)	C24—H24B	0.9800
F4—C26	1.344 (9)	C24—H24C	0.9800

C3—S1—C1	100.0 (2)	F2—C25—F3	106.7 (4)
C3—N1—C4	109.1 (4)	F1—C25—S3	112.2 (3)
C3—N1—C2	125.2 (5)	F2—C25—S3	112.5 (4)
C4—N1—C2	125.4 (4)	F3—C25—S3	111.7 (4)
S1—C1—H1A	109.5	C15—C10—C11	121.8 (4)
S1—C1—H1AB	109.5	C15—C10—N2	119.8 (4)
H1A—C1—H1AB	109.5	C11—C10—N2	118.5 (4)
S1—C1—H1AC	109.5	C12—C13—C14	119.0 (4)
H1A—C1—H1AC	109.5	C12—C13—H13	120.5
H1AB—C1—H1AC	109.5	C14—C13—H13	120.5
N1—C2—H2A	109.5	C13—C12—C11	120.8 (4)
N1—C2—H2AB	109.5	C13—C12—H12	119.6
H2A—C2—H2AB	109.5	C11—C12—H12	119.6
N1—C2—H2AC	109.5	C12—C11—C10	118.7 (4)
H2A—C2—H2AC	109.5	C12—C11—H11	120.6
H2AB—C2—H2AC	109.5	C10—C11—H11	120.6
C23—S2—C24	101.6 (3)	C10—C15—C14	117.7 (4)
C3—N2—C9	109.2 (4)	C10—C15—H15	121.1
C3—N2—C10	125.9 (4)	C14—C15—H15	121.1
C9—N2—C10	124.3 (4)	C13—C14—C15	122.0 (4)

O2—S3—O1	114.5 (3)	C13—C14—N3	120.0 (4)
O2—S3—O3	114.3 (3)	C15—C14—N3	117.9 (4)
O1—S3—O3	116.2 (3)	C17—C16—C21	123.1 (4)
O2—S3—C25	104.0 (3)	C17—C16—N3	130.9 (4)
O1—S3—C25	103.2 (2)	C21—C16—N3	106.0 (4)
O3—S3—C25	102.2 (2)	C16—C17—C18	115.5 (5)
C23—N3—C16	108.7 (4)	C16—C17—H17	122.2
C23—N3—C14	125.8 (4)	C18—C17—H17	122.2
C16—N3—C14	124.7 (4)	C17—C18—C19	121.3 (6)
N2—C3—N1	108.6 (4)	C17—C18—H18	119.4
N2—C3—S1	124.8 (3)	C19—C18—H18	119.4
N1—C3—S1	126.6 (4)	C20—C19—C18	122.7 (5)
N1—C4—C9	107.9 (4)	C20—C19—H19	118.6
N1—C4—C5	132.3 (5)	C18—C19—H19	118.6
C9—C4—C5	119.7 (5)	F5—C26—F4	109.5 (8)
O4—S4—O6	113.6 (3)	F5—C26—F6	107.5 (9)
O4—S4—O5	115.7 (3)	F4—C26—F6	104.6 (9)
O6—S4—O5	116.3 (3)	F5—C26—S4	114.0 (8)
O4—S4—C26	102.7 (5)	F4—C26—S4	111.1 (6)
O6—S4—C26	102.4 (3)	F6—C26—S4	109.6 (6)
O5—S4—C26	103.4 (4)	C19—C20—C21	115.9 (5)
C23—N4—C21	108.8 (4)	C19—C20—H20	122.0
C23—N4—C22	126.0 (5)	C21—C20—H20	122.0
C21—N4—C22	125.1 (4)	N4—C21—C16	107.9 (4)
C6—C5—C4	116.6 (5)	N4—C21—C20	130.7 (5)
C6—C5—H5	121.7	C16—C21—C20	121.4 (5)
C4—C5—H5	121.7	N4—C22—H22A	109.5
C5—C6—C7	123.2 (5)	N4—C22—H22B	109.5
C5—C6—H6	118.4	H22A—C22—H22B	109.5
C7—C6—H6	118.4	N4—C22—H22C	109.5
C8—C7—C6	121.1 (6)	H22A—C22—H22C	109.5
C8—C7—H7	119.5	H22B—C22—H22C	109.5
C6—C7—H7	119.5	N3—C23—N4	108.6 (4)
C9—C8—C7	115.8 (5)	N3—C23—S2	126.5 (3)
C9—C8—H8	122.1	N4—C23—S2	124.7 (4)
C7—C8—H8	122.1	S2—C24—H24A	109.5
C8—C9—C4	123.6 (4)	S2—C24—H24B	109.5
C8—C9—N2	131.0 (4)	H24A—C24—H24B	109.5
C4—C9—N2	105.3 (4)	S2—C24—H24C	109.5
F1—C25—F2	106.9 (5)	H24A—C24—H24C	109.5
F1—C25—F3	106.3 (4)	H24B—C24—H24C	109.5

3,3′-Bis(methylselanyl)-1,1′-(1,3-phenylene)bis(1*H*-1,3-benzodiazol-3-ium) bis(trifluoromethanesulfonate) 1,2-dichloroethane hemisolvate (TS-056_3Se-C)

Crystal data

$C_{24}H_{24}N_4Se_2^{2+}\cdot 2CF_3O_3S^-\cdot 0.5C_2H_4Cl_2$
M_r = 874.01
Triclinic, $P\overline{1}$
a = 9.3672 (1) Å
b = 13.3265 (2) Å
c = 13.6445 (1) Å
α = 102.515 (1)°
β = 93.231 (1)°
γ = 96.198 (1)°
V = 1647.49 (3) Å^3
Z = 2
$F(000)$ = 870
D_x = 1.762 Mg m^{-3}
Cu $K\alpha$ radiation, λ = 1.54184 Å
Cell parameters from 5795 reflections
θ = 3.3–66.5°
μ = 5.48 mm^{-1}
T = 170 K
Cut plate, translucent colourless
0.19 × 0.10 × 0.08 mm

Data collection

Rigaku XtaLAB Synergy Dualflex diffractometer with a HyPix detector
Radiation source: micro-focus sealed X-ray tube, PhotonJet (Cu) X-ray Source
Mirror monochromator
ω scans
Absorption correction: gaussian (CrysAlis PRO; Rigaku OD, 2018)
T_{min} = 0.456, T_{max} = 1.000
19605 measured reflections
5795 independent reflections
5307 reflections with $I > 2\sigma(I)$
R_{int} = 0.046
θ_{max} = 66.5°, θ_{min} = 3.3°
h = −11→10
k = −15→15
l = −14→16

Refinement

Refinement on F^2
Least-squares matrix: full
$R[F^2 > 2\sigma(F^2)]$ = 0.048
$wR(F^2)$ = 0.127
S = 1.05
5795 reflections
484 parameters
28 restraints
Hydrogen site location: inferred from neighbouring sites
H-atom parameters constrained
$w = 1/[\sigma^2(F_o^2) + (0.0607P)^2 + 3.3756P]$ where $P = (F_o^2 + 2F_c^2)/3$
$(\Delta/\sigma)_{max}$ = 0.001
$\Delta\rho_{max}$ = 0.84 e Å^{-3}
$\Delta\rho_{min}$ = −0.79 e Å^{-3}

Special details

Geometry. All e.s.d.'s (except the e.s.d. in the dihedral angle between two l.s. planes) are estimated using the full covariance matrix. The cell e.s.d.'s are taken into account individually in the estimation of e.s.d.'s in distances, angles and torsion angles; correlations between e.s.d.'s in cell parameters are only used when they are defined by crystal symmetry. An approximate (isotropic) treatment of cell e.s.d.'s is used for estimating e.s.d.'s involving l.s. planes.
Refinement. Due to a 95:5 disorder of one the benzimidazolium rings and a shift issue involving N1B, the atom was fixed at 0.314376 0.678949 0.447267

Fractional atomic coordinates and isotropic or equivalent isotropic displacement parameters (Å²)

	x	*y*	*z*	U_{iso}*/U_{eq}	Occ. (<1)
Se1A	0.51229 (5)	0.78078 (3)	0.20663 (3)	0.03655 (15)	0.9498 (10)
N1A	0.3629 (6)	0.7664 (3)	0.3822 (3)	0.0317 (8)	0.9498 (10)
N2A	0.4146 (11)	0.6162 (3)	0.3040 (4)	0.0261 (7)	0.9498 (10)
C1A	0.7037 (5)	0.7379 (4)	0.2166 (3)	0.0420 (10)	0.9498 (10)
H1AA	0.764582	0.768208	0.171733	0.063*	0.9498 (10)

H1AB	0.696569	0.662222	0.196995	0.063*	0.9498 (10)
H1AC	0.746273	0.761771	0.286196	0.063*	0.9498 (10)
C3A	0.4277 (7)	0.7173 (3)	0.3041 (3)	0.0282 (10)	0.9498 (10)
C4A	0.3515 (9)	0.8774 (4)	0.4098 (6)	0.0499 (17)	0.9498 (10)
H4AA	0.360353	0.900770	0.483322	0.075*	0.9498 (10)
H4AB	0.257903	0.890591	0.382867	0.075*	0.9498 (10)
H4AC	0.428760	0.915132	0.381636	0.075*	0.9498 (10)
C5A	0.3027 (4)	0.6943 (3)	0.4323 (3)	0.0315 (8)	0.9498 (10)
C6A	0.2161 (5)	0.7041 (4)	0.5138 (3)	0.0423 (11)	0.9498 (10)
H6A	0.190937	0.769239	0.547424	0.051*	0.9498 (10)
C7A	0.1696 (5)	0.6134 (4)	0.5419 (3)	0.0455 (11)	0.9498 (10)
H7A	0.108846	0.616114	0.595601	0.055*	0.9498 (10)
C8A	0.2087 (5)	0.5180 (4)	0.4944 (5)	0.0421 (12)	0.9498 (10)
H8A	0.176484	0.458318	0.518278	0.051*	0.9498 (10)
C9A	0.2924 (4)	0.5074 (3)	0.4139 (3)	0.0341 (9)	0.9498 (10)
H9A	0.317749	0.442275	0.380633	0.041*	0.9498 (10)
C10A	0.3373 (5)	0.5987 (4)	0.3846 (3)	0.0283 (11)	0.9498 (10)
Se1B	0.3520 (10)	0.4679 (6)	0.4492 (6)	0.03655 (15)	0.0502 (10)
C1B	0.170 (9)	0.503 (11)	0.499 (13)	0.0420 (10)	0.0502 (10)
H1BA	0.154002	0.571836	0.488350	0.063*	0.0502 (10)
H1BB	0.171045	0.503692	0.570562	0.063*	0.0502 (10)
H1BC	0.091254	0.451706	0.461725	0.063*	0.0502 (10)
N1B	0.314376	0.678949	0.447267	0.0317 (8)	0.0502 (10)
N2B	0.41 (2)	0.604 (4)	0.312 (8)	0.0261 (7)	0.0502 (10)
C3B	0.359 (15)	0.590 (4)	0.400 (5)	0.0282 (10)	0.0502 (10)
C4B	0.262 (13)	0.702 (6)	0.547 (4)	0.0499 (17)	0.0502 (10)
H4BA	0.267257	0.777660	0.571149	0.075*	0.0502 (10)
H4BB	0.320596	0.674078	0.593420	0.075*	0.0502 (10)
H4BC	0.161140	0.671305	0.543359	0.075*	0.0502 (10)
C5B	0.341 (16)	0.762 (5)	0.403 (8)	0.0315 (8)	0.0502 (10)
C6B	0.322 (19)	0.867 (6)	0.417 (9)	0.0423 (11)	0.0502 (10)
H6B	0.282495	0.904160	0.474158	0.051*	0.0502 (10)
C7B	0.366 (9)	0.912 (4)	0.340 (5)	0.0455 (11)	0.0502 (10)
H7B	0.340495	0.978647	0.338420	0.055*	0.0502 (10)
C8B	0.446 (8)	0.864 (4)	0.264 (4)	0.0421 (12)	0.0502 (10)
H8B	0.482276	0.901547	0.216517	0.051*	0.0502 (10)
C9B	0.474 (8)	0.763 (4)	0.257 (5)	0.0341 (9)	0.0502 (10)
H9B	0.532521	0.731073	0.207871	0.041*	0.0502 (10)
C10B	0.413 (16)	0.712 (4)	0.325 (8)	0.0283 (11)	0.0502 (10)
C2A	0.9577 (5)	0.5809 (3)	0.2775 (3)	0.0440 (10)	
H2AA	1.000622	0.651134	0.276882	0.066*	
H2AB	1.022288	0.549576	0.317907	0.066*	
H2AC	0.864711	0.583860	0.306753	0.066*	
N3	0.7211 (3)	0.3466 (2)	0.1936 (2)	0.0279 (6)	
N4	0.9361 (3)	0.2978 (2)	0.1916 (2)	0.0311 (6)	
Se2	0.92896 (4)	0.49697 (3)	0.13920 (3)	0.03528 (14)	
C11	0.8597 (4)	0.3727 (3)	0.1769 (3)	0.0293 (7)	
C12	1.0894 (4)	0.2924 (4)	0.1769 (3)	0.0410 (9)	

H12A	1.139658	0.284118	0.239078	0.062*	
H12B	1.131541	0.356278	0.159712	0.062*	
H12C	1.099365	0.233066	0.122044	0.062*	
C13	0.8453 (4)	0.2191 (3)	0.2166 (3)	0.0312 (8)	
C14	0.8724 (5)	0.1257 (3)	0.2395 (3)	0.0389 (9)	
H14	0.965944	0.104311	0.238527	0.047*	
C15	0.7561 (5)	0.0660 (3)	0.2636 (3)	0.0443 (10)	
H15	0.769564	0.001151	0.278621	0.053*	
C16	0.6181 (5)	0.0981 (3)	0.2668 (3)	0.0445 (10)	
H16	0.541410	0.054914	0.285092	0.053*	
C17	0.5906 (5)	0.1913 (3)	0.2439 (3)	0.0384 (9)	
H17	0.497432	0.213314	0.245928	0.046*	
C18	0.7082 (4)	0.2503 (3)	0.2177 (3)	0.0310 (8)	
C19	0.4537 (4)	0.5337 (3)	0.2273 (2)	0.0260 (7)	
C20	0.3729 (4)	0.5062 (3)	0.1355 (3)	0.0321 (8)	
H20	0.295222	0.542871	0.122199	0.039*	
C21	0.4075 (5)	0.4237 (3)	0.0631 (3)	0.0385 (9)	
H21	0.351792	0.402888	0.000176	0.046*	
C22	0.5228 (4)	0.3717 (3)	0.0820 (3)	0.0332 (8)	
H22	0.547201	0.315945	0.032132	0.040*	
C23	0.6021 (4)	0.4021 (3)	0.1748 (3)	0.0279 (7)	
C24	0.5678 (4)	0.4821 (3)	0.2498 (3)	0.0270 (7)	
H24	0.620428	0.500739	0.313983	0.032*	
S1	0.11819 (10)	0.75468 (7)	0.09579 (7)	0.0331 (2)	
F1	0.2088 (4)	0.9489 (3)	0.1760 (3)	0.0861 (12)	
F2	−0.0039 (4)	0.8998 (3)	0.2082 (3)	0.0947 (14)	
F3	0.0356 (5)	0.9246 (3)	0.0616 (4)	0.1094 (15)	
O1	0.1765 (4)	0.7316 (3)	0.1871 (2)	0.0558 (8)	
O2	0.2189 (3)	0.7585 (3)	0.0206 (2)	0.0495 (8)	
O3	−0.0227 (4)	0.7008 (3)	0.0599 (2)	0.0528 (8)	
C25	0.0879 (6)	0.8895 (4)	0.1370 (5)	0.0594 (13)	
F4	0.0437 (4)	0.1670 (4)	0.5413 (5)	0.126 (2)	
F5	0.2090 (5)	0.0786 (3)	0.5591 (3)	0.0908 (12)	
F6	0.0937 (4)	0.0531 (2)	0.4146 (3)	0.0793 (10)	
C26	0.1483 (5)	0.1260 (4)	0.4950 (4)	0.0552 (12)	
Cl1A	0.352 (2)	0.1088 (13)	−0.0121 (18)	0.062 (2)	0.574 (10)
C27A	0.5136 (10)	0.0490 (7)	−0.0184 (7)	0.0509 (18)	0.574 (10)
H27A	0.540977	0.033300	−0.088571	0.061*	0.574 (10)
H27B	0.593142	0.096079	0.024336	0.061*	0.574 (10)
Cl1B	0.345 (3)	0.1106 (19)	0.003 (2)	0.067 (5)	0.426 (10)
C27B	0.4228 (14)	−0.0051 (10)	0.0141 (9)	0.0509 (18)	0.426 (10)
H27C	0.420525	−0.014172	0.084101	0.061*	0.426 (10)
H27D	0.366556	−0.066503	−0.031233	0.061*	0.426 (10)
S2A	0.2594 (6)	0.2311 (5)	0.4639 (5)	0.0436 (9)	0.480 (4)
O4A	0.3166 (4)	0.2966 (3)	0.5527 (3)	0.0635 (7)	0.480 (4)
O5A	0.1604 (10)	0.2659 (6)	0.4004 (6)	0.0635 (7)	0.480 (4)
O6A	0.3731 (9)	0.1796 (7)	0.4160 (6)	0.0635 (7)	0.480 (4)
S2B	0.2967 (6)	0.2109 (5)	0.4596 (5)	0.0436 (9)	0.520 (4)

O4B	0.3166 (4)	0.2966 (3)	0.5527 (3)	0.0635 (7)	0.520 (4)
O5B	0.2447 (9)	0.2429 (6)	0.3721 (5)	0.0635 (7)	0.520 (4)
O6B	0.4035 (8)	0.1392 (6)	0.4430 (6)	0.0635 (7)	0.520 (4)

Atomic displacement parameters (Å²)

	U^{11}	U^{22}	U^{33}	U^{12}	U^{13}	U^{23}
Se1A	0.0403 (3)	0.0340 (2)	0.0387 (3)	0.00902 (18)	0.00641 (19)	0.01247 (18)
N1A	0.039 (3)	0.0313 (17)	0.024 (2)	0.0121 (15)	0.0022 (16)	−0.0016 (14)
N2A	0.0257 (19)	0.0271 (16)	0.0244 (18)	0.007 (2)	0.0029 (13)	0.0012 (13)
C1A	0.034 (2)	0.052 (3)	0.041 (2)	0.0068 (19)	0.0057 (18)	0.010 (2)
C3A	0.031 (2)	0.0296 (19)	0.023 (3)	0.0095 (16)	−0.0001 (19)	0.0020 (15)
C4A	0.072 (6)	0.033 (2)	0.045 (3)	0.020 (3)	0.013 (3)	0.000 (2)
C5A	0.036 (2)	0.036 (2)	0.0205 (17)	0.0099 (16)	−0.0002 (15)	0.0009 (15)
C6A	0.047 (3)	0.052 (3)	0.0261 (19)	0.018 (2)	0.0065 (18)	−0.0009 (19)
C7A	0.052 (3)	0.059 (3)	0.026 (2)	0.011 (2)	0.0114 (18)	0.0076 (19)
C8A	0.042 (3)	0.056 (3)	0.030 (2)	0.003 (3)	0.005 (3)	0.014 (2)
C9A	0.035 (2)	0.043 (2)	0.0261 (18)	0.0103 (18)	0.0059 (16)	0.0080 (17)
C10A	0.026 (3)	0.035 (2)	0.0219 (19)	0.0076 (15)	−0.0016 (18)	0.0020 (15)
Se1B	0.0403 (3)	0.0340 (2)	0.0387 (3)	0.00902 (18)	0.00641 (19)	0.01247 (18)
C1B	0.034 (2)	0.052 (3)	0.041 (2)	0.0068 (19)	0.0057 (18)	0.010 (2)
N1B	0.039 (3)	0.0313 (17)	0.024 (2)	0.0121 (15)	0.0022 (16)	−0.0016 (14)
N2B	0.0257 (19)	0.0271 (16)	0.0244 (18)	0.007 (2)	0.0029 (13)	0.0012 (13)
C3B	0.031 (2)	0.0296 (19)	0.023 (3)	0.0095 (16)	−0.0001 (19)	0.0020 (15)
C4B	0.072 (6)	0.033 (2)	0.045 (3)	0.020 (3)	0.013 (3)	0.000 (2)
C5B	0.036 (2)	0.036 (2)	0.0205 (17)	0.0099 (16)	−0.0002 (15)	0.0009 (15)
C6B	0.047 (3)	0.052 (3)	0.0261 (19)	0.018 (2)	0.0065 (18)	−0.0009 (19)
C7B	0.052 (3)	0.059 (3)	0.026 (2)	0.011 (2)	0.0114 (18)	0.0076 (19)
C8B	0.042 (3)	0.056 (3)	0.030 (2)	0.003 (3)	0.005 (3)	0.014 (2)
C9B	0.035 (2)	0.043 (2)	0.0261 (18)	0.0103 (18)	0.0059 (16)	0.0080 (17)
C10B	0.026 (3)	0.035 (2)	0.0219 (19)	0.0076 (15)	−0.0016 (18)	0.0020 (15)
C2A	0.046 (2)	0.042 (2)	0.041 (2)	−0.0025 (18)	−0.0002 (18)	0.0067 (18)
N3	0.0314 (15)	0.0262 (14)	0.0275 (14)	0.0103 (12)	0.0057 (12)	0.0047 (12)
N4	0.0321 (16)	0.0347 (16)	0.0270 (15)	0.0106 (13)	0.0031 (12)	0.0047 (12)
Se2	0.0374 (2)	0.0349 (2)	0.0354 (2)	0.00516 (17)	0.00790 (17)	0.01026 (17)
C11	0.0319 (19)	0.0328 (18)	0.0234 (16)	0.0108 (15)	0.0035 (14)	0.0034 (14)
C12	0.031 (2)	0.056 (2)	0.040 (2)	0.0166 (18)	0.0052 (16)	0.0129 (19)
C13	0.038 (2)	0.0320 (18)	0.0228 (16)	0.0098 (15)	0.0053 (14)	0.0021 (14)
C14	0.052 (2)	0.035 (2)	0.0325 (19)	0.0177 (18)	0.0041 (17)	0.0075 (16)
C15	0.063 (3)	0.030 (2)	0.042 (2)	0.0132 (19)	0.005 (2)	0.0083 (17)
C16	0.059 (3)	0.033 (2)	0.043 (2)	0.0037 (19)	0.010 (2)	0.0096 (17)
C17	0.041 (2)	0.036 (2)	0.039 (2)	0.0075 (17)	0.0107 (17)	0.0066 (17)
C18	0.037 (2)	0.0283 (18)	0.0274 (17)	0.0098 (15)	0.0043 (15)	0.0035 (14)
C19	0.0274 (17)	0.0256 (17)	0.0240 (16)	0.0052 (13)	0.0058 (13)	0.0016 (13)
C20	0.0301 (18)	0.0360 (19)	0.0307 (18)	0.0115 (15)	0.0012 (14)	0.0051 (15)
C21	0.043 (2)	0.045 (2)	0.0257 (18)	0.0138 (18)	−0.0031 (15)	−0.0003 (16)
C22	0.042 (2)	0.0320 (18)	0.0233 (17)	0.0101 (16)	0.0033 (15)	−0.0009 (14)
C23	0.0307 (18)	0.0273 (17)	0.0278 (17)	0.0083 (14)	0.0079 (14)	0.0072 (14)

C24	0.0299 (17)	0.0265 (17)	0.0238 (16)	0.0056 (14)	0.0028 (13)	0.0030 (13)
S1	0.0357 (5)	0.0350 (5)	0.0303 (4)	0.0125 (4)	0.0068 (4)	0.0064 (4)
F1	0.083 (2)	0.0558 (18)	0.100 (3)	−0.0195 (17)	0.032 (2)	−0.0168 (18)
F2	0.080 (2)	0.0578 (19)	0.137 (3)	0.0152 (17)	0.065 (2)	−0.015 (2)
F3	0.117 (3)	0.078 (3)	0.158 (4)	0.041 (2)	0.002 (3)	0.069 (3)
O1	0.0515 (19)	0.080 (2)	0.0465 (17)	0.0198 (17)	0.0052 (14)	0.0311 (17)
O2	0.0509 (18)	0.064 (2)	0.0327 (15)	0.0124 (15)	0.0140 (13)	0.0042 (14)
O3	0.0496 (18)	0.0523 (18)	0.0515 (18)	−0.0028 (15)	−0.0018 (14)	0.0069 (15)
C25	0.054 (3)	0.046 (3)	0.080 (4)	0.009 (2)	0.021 (3)	0.012 (3)
F4	0.065 (2)	0.098 (3)	0.198 (5)	0.003 (2)	0.051 (3)	−0.012 (3)
F5	0.149 (4)	0.062 (2)	0.063 (2)	0.008 (2)	−0.008 (2)	0.0237 (16)
F6	0.092 (2)	0.0539 (18)	0.079 (2)	−0.0090 (17)	−0.0269 (19)	0.0038 (16)
C26	0.050 (3)	0.042 (2)	0.067 (3)	0.011 (2)	−0.004 (2)	−0.003 (2)
Cl1A	0.072 (5)	0.056 (3)	0.057 (3)	−0.002 (3)	0.008 (3)	0.016 (2)
C27A	0.054 (5)	0.048 (5)	0.048 (3)	−0.006 (3)	0.008 (4)	0.009 (3)
Cl1B	0.061 (4)	0.063 (5)	0.078 (12)	0.016 (4)	0.013 (5)	0.015 (5)
C27B	0.054 (5)	0.048 (5)	0.048 (3)	−0.006 (3)	0.008 (4)	0.009 (3)
S2A	0.044 (3)	0.053 (2)	0.0337 (7)	0.0048 (14)	0.0019 (15)	0.0100 (13)
O4A	0.0682 (17)	0.0675 (17)	0.0527 (15)	−0.0037 (14)	−0.0107 (12)	0.0189 (12)
O5A	0.0682 (17)	0.0675 (17)	0.0527 (15)	−0.0037 (14)	−0.0107 (12)	0.0189 (12)
O6A	0.0682 (17)	0.0675 (17)	0.0527 (15)	−0.0037 (14)	−0.0107 (12)	0.0189 (12)
S2B	0.044 (3)	0.053 (2)	0.0337 (7)	0.0048 (14)	0.0019 (15)	0.0100 (13)
O4B	0.0682 (17)	0.0675 (17)	0.0527 (15)	−0.0037 (14)	−0.0107 (12)	0.0189 (12)
O5B	0.0682 (17)	0.0675 (17)	0.0527 (15)	−0.0037 (14)	−0.0107 (12)	0.0189 (12)
O6B	0.0682 (17)	0.0675 (17)	0.0527 (15)	−0.0037 (14)	−0.0107 (12)	0.0189 (12)

Geometric parameters (Å, º)

Se1A—C3A	1.891 (4)	N3—C23	1.444 (5)
Se1A—C1A	1.946 (4)	N4—C11	1.331 (5)
N1A—C3A	1.338 (5)	N4—C13	1.391 (5)
N1A—C5A	1.386 (5)	N4—C12	1.468 (5)
N1A—C4A	1.461 (5)	Se2—C11	1.899 (4)
N2A—C3A	1.339 (5)	C12—H12A	0.9800
N2A—C10A	1.397 (6)	C12—H12B	0.9800
N2A—C19	1.439 (4)	C12—H12C	0.9800
C1A—H1AA	0.9800	C13—C18	1.392 (5)
C1A—H1AB	0.9800	C13—C14	1.393 (5)
C1A—H1AC	0.9800	C14—C15	1.376 (7)
C4A—H4AA	0.9800	C14—H14	0.9500
C4A—H4AB	0.9800	C15—C16	1.405 (7)
C4A—H4AC	0.9800	C15—H15	0.9500
C5A—C10A	1.382 (6)	C16—C17	1.391 (6)
C5A—C6A	1.404 (6)	C16—H16	0.9500
C6A—C7A	1.380 (7)	C17—C18	1.392 (6)
C6A—H6A	0.9500	C17—H17	0.9500
C7A—C8A	1.393 (8)	C19—C20	1.382 (5)
C7A—H7A	0.9500	C19—C24	1.386 (5)

C8A—C9A	1.376 (7)	C20—C21	1.389 (5)
C8A—H8A	0.9500	C20—H20	0.9500
C9A—C10A	1.391 (7)	C21—C22	1.386 (6)
C9A—H9A	0.9500	C21—H21	0.9500
Se1B—C3B	1.89 (2)	C22—C23	1.387 (5)
Se1B—C1B	1.94 (2)	C22—H22	0.9500
C1B—H1BA	0.9800	C23—C24	1.387 (5)
C1B—H1BB	0.9800	C24—H24	0.9500
C1B—H1BC	0.9800	S1—O2	1.437 (3)
N1B—C3B	1.337 (19)	S1—O3	1.437 (3)
N1B—C5B	1.38 (2)	S1—O1	1.439 (3)
N1B—C4B	1.455 (18)	S1—C25	1.821 (5)
N2B—C3B	1.35 (2)	F1—C25	1.323 (6)
N2B—C10B	1.40 (2)	F2—C25	1.328 (6)
N2B—C19	1.446 (16)	F3—C25	1.310 (7)
C4B—H4BA	0.9800	F4—C26	1.301 (6)
C4B—H4BB	0.9800	F5—C26	1.322 (6)
C4B—H4BC	0.9800	F6—C26	1.333 (6)
C5B—C10B	1.38 (2)	C26—S2A	1.794 (9)
C5B—C6B	1.41 (2)	C26—S2B	1.850 (8)
C6B—C7B	1.37 (2)	Cl1A—C27A	1.78 (2)
C6B—H6B	0.9500	C27A—C27A^{i}	1.499 (18)
C7B—C8B	1.40 (2)	C27A—H27A	0.9900
C7B—H7B	0.9500	C27A—H27B	0.9900
C8B—C9B	1.38 (2)	Cl1B—C27B	1.81 (3)
C8B—H8B	0.9500	C27B—C27B^{i}	1.52 (3)
C9B—C10B	1.38 (2)	C27B—H27C	0.9900
C9B—H9B	0.9500	C27B—H27D	0.9900
C2A—Se2	1.961 (4)	S2A—O4A	1.372 (8)
C2A—H2AA	0.9800	S2A—O5A	1.415 (8)
C2A—H2AB	0.9800	S2A—O6A	1.441 (9)
C2A—H2AC	0.9800	S2B—O5B	1.430 (8)
N3—C11	1.352 (5)	S2B—O6B	1.451 (8)
N3—C18	1.388 (5)	S2B—O4B	1.500 (7)

C3A—Se1A—C1A	99.1 (2)	N4—C11—N3	108.8 (3)
C3A—N1A—C5A	108.9 (3)	N4—C11—Se2	126.9 (3)
C3A—N1A—C4A	126.5 (4)	N3—C11—Se2	124.2 (3)
C5A—N1A—C4A	124.6 (3)	N4—C12—H12A	109.5
C3A—N2A—C10A	109.4 (3)	N4—C12—H12B	109.5
C3A—N2A—C19	127.2 (3)	H12A—C12—H12B	109.5
C10A—N2A—C19	122.9 (4)	N4—C12—H12C	109.5
Se1A—C1A—H1AA	109.5	H12A—C12—H12C	109.5
Se1A—C1A—H1AB	109.5	H12B—C12—H12C	109.5
H1AA—C1A—H1AB	109.5	N4—C13—C18	106.6 (3)
Se1A—C1A—H1AC	109.5	N4—C13—C14	131.5 (4)
H1AA—C1A—H1AC	109.5	C18—C13—C14	121.9 (4)
H1AB—C1A—H1AC	109.5	C15—C14—C13	116.3 (4)

N1A—C3A—N2A	108.6 (3)	C15—C14—H14	121.9
N1A—C3A—Se1A	124.8 (3)	C13—C14—H14	121.9
N2A—C3A—Se1A	126.5 (3)	C14—C15—C16	122.1 (4)
N1A—C4A—H4AA	109.5	C14—C15—H15	119.0
N1A—C4A—H4AB	109.5	C16—C15—H15	119.0
H4AA—C4A—H4AB	109.5	C17—C16—C15	121.8 (4)
N1A—C4A—H4AC	109.5	C17—C16—H16	119.1
H4AA—C4A—H4AC	109.5	C15—C16—H16	119.1
H4AB—C4A—H4AC	109.5	C16—C17—C18	115.7 (4)
C10A—C5A—N1A	107.4 (4)	C16—C17—H17	122.1
C10A—C5A—C6A	120.9 (4)	C18—C17—H17	122.1
N1A—C5A—C6A	131.7 (4)	N3—C18—C13	106.5 (3)
C7A—C6A—C5A	115.9 (4)	N3—C18—C17	131.3 (3)
C7A—C6A—H6A	122.0	C13—C18—C17	122.2 (3)
C5A—C6A—H6A	122.0	C20—C19—C24	122.5 (3)
C6A—C7A—C8A	122.4 (4)	C20—C19—N2A	118.9 (5)
C6A—C7A—H7A	118.8	C24—C19—N2A	118.6 (5)
C8A—C7A—H7A	118.8	C20—C19—N2B	121 (9)
C9A—C8A—C7A	122.2 (5)	C24—C19—N2B	115 (8)
C9A—C8A—H8A	118.9	C19—C20—C21	118.7 (3)
C7A—C8A—H8A	118.9	C19—C20—H20	120.7
C8A—C9A—C10A	115.4 (4)	C21—C20—H20	120.7
C8A—C9A—H9A	122.3	C22—C21—C20	120.5 (3)
C10A—C9A—H9A	122.3	C22—C21—H21	119.7
C5A—C10A—C9A	123.2 (4)	C20—C21—H21	119.7
C5A—C10A—N2A	105.7 (4)	C21—C22—C23	119.1 (3)
C9A—C10A—N2A	131.0 (4)	C21—C22—H22	120.5
C3B—Se1B—C1B	86 (5)	C23—C22—H22	120.5
Se1B—C1B—H1BA	109.5	C24—C23—C22	121.9 (3)
Se1B—C1B—H1BB	109.5	C24—C23—N3	119.7 (3)
H1BA—C1B—H1BB	109.5	C22—C23—N3	118.4 (3)
Se1B—C1B—H1BC	109.5	C19—C24—C23	117.3 (3)
H1BA—C1B—H1BC	109.5	C19—C24—H24	121.3
H1BB—C1B—H1BC	109.5	C23—C24—H24	121.3
C3B—N1B—C5B	116 (4)	O2—S1—O3	115.94 (19)
C3B—N1B—C4B	128 (3)	O2—S1—O1	114.8 (2)
C5B—N1B—C4B	116 (4)	O3—S1—O1	114.0 (2)
C3B—N2B—C10B	102 (4)	O2—S1—C25	103.0 (2)
C3B—N2B—C19	132 (3)	O3—S1—C25	104.2 (2)
C10B—N2B—C19	126 (4)	O1—S1—C25	102.5 (3)
N1B—C3B—N2B	108.1 (18)	F3—C25—F1	108.3 (5)
N1B—C3B—Se1B	125.1 (18)	F3—C25—F2	108.6 (5)
N2B—C3B—Se1B	127 (3)	F1—C25—F2	106.9 (5)
N1B—C4B—H4BA	109.5	F3—C25—S1	110.9 (4)
N1B—C4B—H4BB	109.5	F1—C25—S1	111.3 (4)
H4BA—C4B—H4BB	109.5	F2—C25—S1	110.7 (4)
N1B—C4B—H4BC	109.5	F4—C26—F5	104.9 (5)
H4BA—C4B—H4BC	109.5	F4—C26—F6	109.4 (5)

H4BB—C4B—H4BC	109.5	F5—C26—F6	107.1 (4)
N1B—C5B—C10B	97 (5)	F4—C26—S2A	105.8 (4)
N1B—C5B—C6B	141 (6)	F5—C26—S2A	116.0 (4)
C10B—C5B—C6B	122 (2)	F6—C26—S2A	113.2 (5)
C7B—C6B—C5B	114 (3)	F4—C26—S2B	119.5 (4)
C7B—C6B—H6B	122.9	F5—C26—S2B	105.5 (4)
C5B—C6B—H6B	122.9	F6—C26—S2B	109.7 (4)
C6B—C7B—C8B	123 (3)	C27A^{i}—C27A—Cl1A	107.9 (10)
C6B—C7B—H7B	118.3	C27A^{i}—C27A—H27A	110.1
C8B—C7B—H7B	118.3	Cl1A—C27A—H27A	110.1
C9B—C8B—C7B	120 (2)	C27A^{i}—C27A—H27B	110.1
C9B—C8B—H8B	119.8	Cl1A—C27A—H27B	110.1
C7B—C8B—H8B	119.8	H27A—C27A—H27B	108.4
C10B—C9B—C8B	117 (2)	C27B^{i}—C27B—Cl1B	108.7 (15)
C10B—C9B—H9B	121.4	C27B^{i}—C27B—H27C	110.0
C8B—C9B—H9B	121.4	Cl1B—C27B—H27C	110.0
C9B—C10B—C5B	121 (3)	C27B^{i}—C27B—H27D	110.0
C9B—C10B—N2B	122 (6)	Cl1B—C27B—H27D	110.0
C5B—C10B—N2B	116 (6)	H27C—C27B—H27D	108.3
Se2—C2A—H2AA	109.5	O4A—S2A—O5A	119.3 (5)
Se2—C2A—H2AB	109.5	O4A—S2A—O6A	108.6 (5)
H2AA—C2A—H2AB	109.5	O5A—S2A—O6A	116.4 (7)
Se2—C2A—H2AC	109.5	O4A—S2A—C26	107.6 (5)
H2AA—C2A—H2AC	109.5	O5A—S2A—C26	100.8 (5)
H2AB—C2A—H2AC	109.5	O6A—S2A—C26	102.0 (5)
C11—N3—C18	108.9 (3)	O5B—S2B—O6B	115.3 (6)
C11—N3—C23	125.6 (3)	O5B—S2B—O4B	113.1 (5)
C18—N3—C23	125.0 (3)	O6B—S2B—O4B	118.8 (5)
C11—N4—C13	109.2 (3)	O5B—S2B—C26	107.5 (5)
C11—N4—C12	126.8 (3)	O6B—S2B—C26	99.5 (5)
C13—N4—C12	123.8 (3)	O4B—S2B—C26	99.5 (4)
C11—Se2—C2A	94.86 (17)		

Symmetry code: (i) $-x+1, -y, -z$.

3,3′-Bis(methylselanyl)-1,1′-(1,3-phenylene)bis(1*H*-1,3-benzodiazol-3-ium) bis(trifluoromethanesulfonate) (TS-056_twin_twin1_hklf4_3Se-B)

Crystal data

$C_{24}H_{24}N_4Se_2^{2+}\cdot 2CF_3O_3S^-$
M_r = 824.53
Monoclinic, $P2_1/c$
a = 13.8634 (4) Å
b = 7.7558 (2) Å
c = 29.3266 (7) Å
β = 94.246 (2)°
V = 3144.59 (14) Å^3
Z = 4
$F(000)$ = 1640
D_x = 1.742 Mg m^{-3}
Cu $K\alpha$ radiation, λ = 1.54184 Å
Cell parameters from 5529 reflections
θ = 3.0–66.5°
μ = 4.93 mm^{-1}
T = 170 K
Needle, clear colourless
0.03 × 0.02 × 0.01 mm

Data collection

Rigaku XtaLAB Synergy Dualflex diffractometer with a HyPix detector
Radiation source: micro-focus sealed X-ray tube, PhotonJet (Cu) X-ray Source
Mirror monochromator
ω scans
Absorption correction: gaussian (CrysAlis PRO; Rigaku OD, 2018)
T_{min} = 0.900, T_{max} = 0.969
28154 measured reflections
5529 independent reflections
4865 reflections with $I > 2\sigma(I)$
R_{int} = 0.073
θ_{max} = 66.5°, θ_{min} = 3.0°
h = −16→16
k = −8→9
l = −34→34

Refinement

Refinement on F^2
Least-squares matrix: full
$R[F^2 > 2\sigma(F^2)]$ = 0.053
$wR(F^2)$ = 0.142
S = 1.06
5529 reflections
419 parameters
0 restraints
Hydrogen site location: inferred from neighbouring sites
H-atom parameters constrained
$w = 1/[\sigma^2(F_o^2) + (0.0737P)^2 + 7.2679P]$ where $P = (F_o^2 + 2F_c^2)/3$
$(\Delta/\sigma)_{max}$ = 0.001
$\Delta\rho_{max}$ = 1.21 e Å^{-3}
$\Delta\rho_{min}$ = −0.84 e Å^{-3}

Special details

Geometry. All e.s.d.'s (except the e.s.d. in the dihedral angle between two l.s. planes) are estimated using the full covariance matrix. The cell e.s.d.'s are taken into account individually in the estimation of e.s.d.'s in distances, angles and torsion angles; correlations between e.s.d.'s in cell parameters are only used when they are defined by crystal symmetry. An approximate (isotropic) treatment of cell e.s.d.'s is used for estimating e.s.d.'s involving l.s. planes.

Refinement. Twin

Fractional atomic coordinates and isotropic or equivalent isotropic displacement parameters (Å^2)

	x	y	z	U_{iso}*/U_{eq}
Se1	0.11263 (3)	0.38325 (5)	0.29868 (2)	0.03215 (15)
F1	0.0959 (2)	0.5093 (5)	0.47848 (13)	0.0694 (9)
N1	−0.0191 (2)	0.2977 (5)	0.36753 (12)	0.0341 (8)
C1	0.0526 (4)	0.2371 (8)	0.25052 (17)	0.0579 (14)
H1A	0.052811	0.296917	0.221099	0.087*
H1AB	−0.014215	0.211641	0.257104	0.087*
H1AC	0.088992	0.129092	0.249142	0.087*
S1	0.25873 (8)	0.56039 (14)	0.19470 (4)	0.0372 (3)
O1	0.3333 (3)	0.5611 (5)	0.23149 (13)	0.0578 (9)
Se2	0.41613 (3)	0.38318 (6)	0.31859 (2)	0.04288 (17)
F2	0.2279 (3)	0.4471 (5)	0.51749 (10)	0.0692 (9)
N2	0.0917 (2)	0.1025 (4)	0.36094 (12)	0.0294 (7)
C2	0.5275 (4)	0.4091 (9)	0.2823 (2)	0.0670 (17)
H2A	0.505489	0.442600	0.251066	0.101*
H2AB	0.562469	0.299384	0.281726	0.101*
H2AC	0.570588	0.498308	0.295994	0.101*
S2	0.25037 (8)	0.53832 (14)	0.43272 (4)	0.0362 (2)
O2	0.2737 (3)	0.6768 (5)	0.15809 (12)	0.0504 (8)
O3	0.1633 (3)	0.5591 (5)	0.20962 (15)	0.0626 (11)
N3	0.4414 (2)	0.0865 (4)	0.37656 (12)	0.0302 (7)

F3	0.1680 (2)	0.2696 (4)	0.46669 (10)	0.0543 (7)
C3	0.0593 (3)	0.2557 (5)	0.34562 (13)	0.0284 (8)
O4	0.2589 (2)	0.7146 (4)	0.44704 (12)	0.0461 (8)
F4	0.2640 (3)	0.2227 (4)	0.19986 (15)	0.0768 (10)
N4	0.5505 (2)	0.2813 (4)	0.39527 (13)	0.0332 (7)
C4	−0.0785 (4)	0.4534 (6)	0.36051 (19)	0.0455 (11)
H4A	−0.056519	0.519097	0.334671	0.068*
H4AB	−0.072162	0.524674	0.388172	0.068*
H4AC	−0.146324	0.420497	0.354010	0.068*
C5	0.4743 (3)	0.2459 (5)	0.36683 (15)	0.0334 (9)
O5	0.1875 (3)	0.5115 (5)	0.39240 (11)	0.0552 (9)
F5	0.3616 (4)	0.3304 (5)	0.15549 (18)	0.1116 (19)
C6	0.6053 (4)	0.4434 (6)	0.39690 (19)	0.0468 (11)
H6A	0.665773	0.427299	0.382119	0.070*
H6AB	0.619983	0.477627	0.428834	0.070*
H6AC	0.566691	0.533656	0.380849	0.070*
O6	0.3386 (3)	0.4417 (5)	0.43480 (14)	0.0567 (9)
F6	0.2080 (5)	0.3186 (6)	0.13605 (17)	0.132 (2)
C7	−0.0375 (3)	0.1685 (6)	0.39801 (15)	0.0352 (9)
C9	−0.1050 (4)	0.0002 (8)	0.4544 (2)	0.0603 (16)
H9	−0.152421	−0.017410	0.475690	0.072*
C8	−0.1085 (4)	0.1495 (7)	0.42879 (18)	0.0503 (12)
H8	−0.156673	0.234819	0.432012	0.060*
C11	0.0402 (3)	−0.1056 (5)	0.42061 (16)	0.0367 (10)
H11	0.091493	−0.186174	0.419121	0.044*
C10	−0.0346 (4)	−0.1258 (8)	0.4502 (2)	0.0582 (15)
H10	−0.037114	−0.228354	0.467791	0.070*
C15	0.6343 (3)	−0.0366 (7)	0.48347 (15)	0.0451 (12)
H15	0.680543	−0.058933	0.508319	0.054*
C14	0.6384 (3)	0.1164 (6)	0.46087 (16)	0.0406 (11)
H14	0.685931	0.201081	0.469317	0.049*
C13	0.5690 (3)	0.1418 (6)	0.42471 (14)	0.0335 (9)
C12	0.0327 (3)	0.0416 (6)	0.39394 (15)	0.0347 (9)
C18	0.4995 (3)	0.0169 (5)	0.41286 (14)	0.0305 (8)
C19	0.2665 (3)	0.0943 (5)	0.36723 (13)	0.0275 (8)
H19	0.267277	0.196541	0.385089	0.033*
C20	0.1806 (3)	0.0211 (5)	0.35003 (13)	0.0290 (8)
C21	0.1784 (3)	−0.1307 (5)	0.32508 (15)	0.0356 (9)
H21	0.118436	−0.180504	0.314207	0.043*
C22	0.2648 (3)	−0.2086 (6)	0.31623 (16)	0.0393 (10)
H22	0.264081	−0.312285	0.298942	0.047*
C23	0.3522 (3)	−0.1372 (5)	0.33229 (15)	0.0345 (9)
H23	0.411477	−0.190701	0.326081	0.041*
C24	0.3520 (3)	0.0128 (5)	0.35743 (13)	0.0286 (8)
C25	0.2726 (5)	0.3490 (7)	0.1695 (2)	0.0605 (15)
C26	0.1816 (3)	0.4383 (6)	0.47555 (15)	0.0348 (9)
C17	0.4944 (3)	−0.1372 (6)	0.43601 (14)	0.0348 (9)
H17	0.445942	−0.220803	0.428141	0.042*

C16	0.5645 (3)	−0.1619 (7)	0.47140 (15)	0.0416 (10)
H16	0.565302	−0.267064	0.488023	0.050*

Atomic displacement parameters (Å²)

	U^{11}	U^{22}	U^{33}	U^{12}	U^{13}	U^{23}
Se1	0.0312 (3)	0.0304 (3)	0.0348 (3)	−0.00345 (16)	0.00218 (18)	0.00444 (17)
F1	0.0504 (18)	0.072 (2)	0.089 (2)	0.0141 (16)	0.0303 (17)	0.0140 (19)
N1	0.0276 (17)	0.0327 (18)	0.0423 (19)	0.0033 (14)	0.0039 (14)	0.0015 (15)
C1	0.062 (3)	0.073 (4)	0.039 (3)	−0.028 (3)	0.001 (2)	−0.001 (3)
S1	0.0404 (6)	0.0362 (6)	0.0363 (5)	−0.0002 (4)	0.0109 (4)	0.0051 (4)
O1	0.068 (2)	0.054 (2)	0.050 (2)	0.0099 (18)	−0.0077 (18)	−0.0003 (17)
Se2	0.0324 (3)	0.0370 (3)	0.0598 (3)	0.00622 (18)	0.0076 (2)	0.0149 (2)
F2	0.082 (2)	0.089 (2)	0.0353 (15)	−0.0044 (19)	−0.0021 (15)	0.0053 (16)
N2	0.0249 (17)	0.0310 (17)	0.0326 (18)	0.0010 (13)	0.0044 (13)	0.0030 (14)
C2	0.054 (3)	0.085 (4)	0.064 (4)	0.014 (3)	0.018 (3)	0.022 (3)
S2	0.0395 (6)	0.0339 (5)	0.0353 (5)	−0.0043 (4)	0.0029 (4)	−0.0009 (4)
O2	0.064 (2)	0.0450 (19)	0.0436 (18)	−0.0139 (17)	0.0129 (16)	0.0093 (15)
O3	0.051 (2)	0.057 (2)	0.084 (3)	0.0100 (18)	0.031 (2)	0.022 (2)
N3	0.0236 (16)	0.0293 (17)	0.0380 (19)	0.0027 (13)	0.0049 (14)	0.0002 (14)
F3	0.0634 (19)	0.0422 (15)	0.0579 (17)	−0.0081 (13)	0.0083 (14)	0.0115 (13)
C3	0.0238 (19)	0.029 (2)	0.032 (2)	−0.0025 (15)	−0.0017 (15)	−0.0026 (16)
O4	0.050 (2)	0.0325 (16)	0.055 (2)	−0.0073 (14)	−0.0011 (15)	−0.0056 (14)
F4	0.088 (3)	0.0385 (17)	0.107 (3)	0.0012 (16)	0.027 (2)	0.0149 (18)
N4	0.0261 (17)	0.0294 (17)	0.045 (2)	−0.0006 (14)	0.0059 (14)	−0.0080 (15)
C4	0.040 (3)	0.037 (2)	0.061 (3)	0.014 (2)	0.009 (2)	0.008 (2)
C5	0.027 (2)	0.030 (2)	0.044 (2)	0.0026 (16)	0.0060 (17)	−0.0021 (18)
O5	0.081 (3)	0.048 (2)	0.0348 (17)	−0.0169 (18)	−0.0084 (16)	0.0041 (15)
F5	0.147 (4)	0.062 (2)	0.140 (4)	0.011 (3)	0.105 (4)	−0.013 (2)
C6	0.040 (3)	0.036 (2)	0.064 (3)	−0.009 (2)	0.005 (2)	−0.014 (2)
O6	0.0429 (19)	0.060 (2)	0.069 (2)	0.0070 (17)	0.0161 (17)	0.0009 (19)
F6	0.222 (7)	0.068 (3)	0.096 (3)	−0.024 (3)	−0.061 (4)	−0.025 (2)
C7	0.027 (2)	0.042 (2)	0.036 (2)	0.0028 (18)	0.0016 (16)	0.0069 (19)
C9	0.038 (3)	0.086 (4)	0.059 (3)	0.012 (3)	0.019 (2)	0.033 (3)
C8	0.035 (2)	0.065 (3)	0.052 (3)	0.012 (2)	0.015 (2)	0.015 (2)
C11	0.033 (2)	0.031 (2)	0.047 (3)	0.0097 (17)	0.0108 (19)	0.0229 (18)
C10	0.046 (3)	0.063 (3)	0.067 (4)	0.007 (2)	0.013 (3)	0.034 (3)
C15	0.033 (2)	0.070 (3)	0.032 (2)	0.015 (2)	0.0021 (18)	−0.003 (2)
C14	0.028 (2)	0.057 (3)	0.037 (2)	0.0027 (19)	0.0040 (18)	−0.012 (2)
C13	0.027 (2)	0.042 (2)	0.033 (2)	0.0059 (17)	0.0090 (16)	−0.0093 (18)
C12	0.0238 (19)	0.042 (2)	0.038 (2)	0.0001 (17)	0.0025 (16)	0.0049 (18)
C18	0.0224 (19)	0.035 (2)	0.035 (2)	0.0060 (16)	0.0073 (15)	−0.0038 (17)
C19	0.029 (2)	0.0250 (18)	0.0284 (19)	−0.0004 (15)	0.0038 (15)	−0.0019 (15)
C20	0.029 (2)	0.0273 (19)	0.031 (2)	0.0016 (15)	0.0051 (15)	0.0024 (16)
C21	0.034 (2)	0.033 (2)	0.040 (2)	−0.0052 (17)	−0.0006 (18)	−0.0044 (17)
C22	0.041 (2)	0.030 (2)	0.047 (3)	−0.0008 (18)	0.0026 (19)	−0.0109 (19)
C23	0.034 (2)	0.031 (2)	0.039 (2)	0.0045 (17)	0.0061 (17)	−0.0039 (17)
C24	0.0268 (19)	0.0282 (19)	0.031 (2)	−0.0002 (15)	0.0018 (15)	0.0015 (16)

C25	0.076 (4)	0.041 (3)	0.067 (4)	−0.009 (3)	0.020 (3)	−0.005 (3)
C26	0.037 (2)	0.034 (2)	0.034 (2)	−0.0011 (18)	0.0050 (17)	0.0015 (17)
C17	0.031 (2)	0.041 (2)	0.034 (2)	0.0081 (17)	0.0078 (17)	0.0015 (18)
C16	0.040 (2)	0.050 (3)	0.036 (2)	0.016 (2)	0.0121 (18)	0.004 (2)

Geometric parameters (Å, º)

Se1—C3	1.890 (4)	C4—H4AC	0.9800
Se1—C1	1.949 (5)	F5—C25	1.337 (8)
F1—C26	1.319 (5)	C6—H6A	0.9800
N1—C3	1.343 (5)	C6—H6AB	0.9800
N1—C7	1.379 (6)	C6—H6AC	0.9800
N1—C4	1.467 (6)	F6—C25	1.300 (8)
C1—H1A	0.9800	C7—C8	1.391 (6)
C1—H1AB	0.9800	C7—C12	1.396 (6)
C1—H1AC	0.9800	C9—C8	1.379 (8)
S1—O3	1.424 (4)	C9—C10	1.393 (8)
S1—O2	1.430 (3)	C9—H9	0.9500
S1—O1	1.438 (4)	C8—H8	0.9500
S1—C25	1.814 (6)	C11—C12	1.383 (6)
Se2—C5	1.901 (4)	C11—C10	1.410 (7)
Se2—C2	1.949 (6)	C11—H11	0.9500
F2—C26	1.346 (5)	C10—H10	0.9500
N2—C3	1.336 (5)	C15—C14	1.362 (7)
N2—C12	1.395 (5)	C15—C16	1.398 (8)
N2—C20	1.442 (5)	C15—H15	0.9500
C2—H2A	0.9800	C14—C13	1.392 (6)
C2—H2AB	0.9800	C14—H14	0.9500
C2—H2AC	0.9800	C13—C18	1.391 (6)
S2—O5	1.431 (4)	C18—C17	1.379 (6)
S2—O6	1.432 (4)	C19—C20	1.381 (6)
S2—O4	1.432 (3)	C19—C24	1.391 (6)
S2—C26	1.807 (4)	C19—H19	0.9500
N3—C5	1.356 (5)	C20—C21	1.385 (6)
N3—C18	1.396 (5)	C21—C22	1.383 (6)
N3—C24	1.440 (5)	C21—H21	0.9500
F3—C26	1.345 (5)	C22—C23	1.383 (6)
F4—C25	1.335 (7)	C22—H22	0.9500
N4—C5	1.326 (6)	C23—C24	1.377 (6)
N4—C13	1.396 (6)	C23—H23	0.9500
N4—C6	1.468 (6)	C17—C16	1.382 (6)
C4—H4A	0.9800	C17—H17	0.9500
C4—H4AB	0.9800	C16—H16	0.9500
C3—Se1—C1	93.1 (2)	C10—C9—H9	118.7
C3—N1—C7	109.2 (3)	C9—C8—C7	116.4 (5)
C3—N1—C4	126.7 (4)	C9—C8—H8	121.8
C7—N1—C4	124.1 (4)	C7—C8—H8	121.8

Se1—C1—H1A	109.5	C12—C11—C10	114.3 (4)
Se1—C1—H1AB	109.5	C12—C11—H11	122.8
H1A—C1—H1AB	109.5	C10—C11—H11	122.8
Se1—C1—H1AC	109.5	C9—C10—C11	121.9 (5)
H1A—C1—H1AC	109.5	C9—C10—H10	119.1
H1AB—C1—H1AC	109.5	C11—C10—H10	119.1
O3—S1—O2	115.1 (2)	C14—C15—C16	122.3 (4)
O3—S1—O1	113.7 (3)	C14—C15—H15	118.8
O2—S1—O1	115.1 (2)	C16—C15—H15	118.8
O3—S1—C25	104.3 (3)	C15—C14—C13	116.3 (4)
O2—S1—C25	103.8 (2)	C15—C14—H14	121.9
O1—S1—C25	102.5 (3)	C13—C14—H14	121.9
C5—Se2—C2	98.9 (2)	C18—C13—C14	121.2 (4)
C3—N2—C12	109.5 (3)	C18—C13—N4	107.0 (4)
C3—N2—C20	125.9 (3)	C14—C13—N4	131.7 (4)
C12—N2—C20	124.1 (3)	C11—C12—N2	130.4 (4)
Se2—C2—H2A	109.5	C11—C12—C7	123.9 (4)
Se2—C2—H2AB	109.5	N2—C12—C7	105.6 (4)
H2A—C2—H2AB	109.5	C17—C18—C13	122.7 (4)
Se2—C2—H2AC	109.5	C17—C18—N3	131.5 (4)
H2A—C2—H2AC	109.5	C13—C18—N3	105.8 (4)
H2AB—C2—H2AC	109.5	C20—C19—C24	117.5 (4)
O5—S2—O6	115.2 (3)	C20—C19—H19	121.2
O5—S2—O4	114.4 (2)	C24—C19—H19	121.2
O6—S2—O4	115.8 (2)	C19—C20—C21	121.8 (4)
O5—S2—C26	101.0 (2)	C19—C20—N2	117.9 (3)
O6—S2—C26	103.8 (2)	C21—C20—N2	120.2 (4)
O4—S2—C26	104.0 (2)	C22—C21—C20	119.0 (4)
C5—N3—C18	109.2 (3)	C22—C21—H21	120.5
C5—N3—C24	125.0 (3)	C20—C21—H21	120.5
C18—N3—C24	125.2 (3)	C21—C22—C23	120.7 (4)
N2—C3—N1	108.6 (3)	C21—C22—H22	119.7
N2—C3—Se1	124.8 (3)	C23—C22—H22	119.7
N1—C3—Se1	126.5 (3)	C24—C23—C22	118.9 (4)
C5—N4—C13	109.3 (3)	C24—C23—H23	120.5
C5—N4—C6	125.7 (4)	C22—C23—H23	120.5
C13—N4—C6	125.0 (4)	C23—C24—C19	122.0 (4)
N1—C4—H4A	109.5	C23—C24—N3	120.5 (4)
N1—C4—H4AB	109.5	C19—C24—N3	117.4 (3)
H4A—C4—H4AB	109.5	F6—C25—F4	106.2 (5)
N1—C4—H4AC	109.5	F6—C25—F5	110.4 (6)
H4A—C4—H4AC	109.5	F4—C25—F5	104.8 (5)
H4AB—C4—H4AC	109.5	F6—C25—S1	112.6 (5)
N4—C5—N3	108.7 (4)	F4—C25—S1	112.0 (4)
N4—C5—Se2	128.8 (3)	F5—C25—S1	110.5 (4)
N3—C5—Se2	122.5 (3)	F1—C26—F3	107.7 (4)
N4—C6—H6A	109.5	F1—C26—F2	106.9 (4)
N4—C6—H6AB	109.5	F3—C26—F2	106.1 (4)

H6A—C6—H6AB	109.5	F1—C26—S2	113.0 (3)
N4—C6—H6AC	109.5	F3—C26—S2	110.9 (3)
H6A—C6—H6AC	109.5	F2—C26—S2	111.9 (3)
H6AB—C6—H6AC	109.5	C18—C17—C16	115.5 (4)
N1—C7—C8	132.2 (4)	C18—C17—H17	122.2
N1—C7—C12	107.0 (4)	C16—C17—H17	122.2
C8—C7—C12	120.8 (4)	C17—C16—C15	121.9 (5)
C8—C9—C10	122.5 (5)	C17—C16—H16	119.0
C8—C9—H9	118.7	C15—C16—H16	119.0

3,3′-Bis(methylselanyl)-1,1′-(1,3-phenylene)bis(1*H*-1,3-benzodiazol-3-ium) bis(trifluoromethanesulfonate) (TS-058_3Se_A)

Crystal data

$C_{24}H_{24}N_4Se_2^{2+}\cdot 2CF_3O_3S^-$
$M_r = 824.53$
Monoclinic, $P2_1/c$
$a = 7.74775$ (4) Å
$b = 13.12863$ (8) Å
$c = 31.27496$ (18) Å
$\beta = 90.6141$ (5)°
$V = 3181.02$ (3) Å^3
$Z = 4$
$F(000) = 1640$
$D_x = 1.722$ Mg m^{-3}
Cu $K\alpha$ radiation, $\lambda = 1.54184$ Å
Cell parameters from 5613 reflections
$\theta = 2.8$–66.5°
$\mu = 4.88$ mm^{-1}
$T = 170$ K
Cut prism, clear colourless
0.29 × 0.14 × 0.08 mm

Data collection

Rigaku XtaLAB Synergy Dualflex diffractometer with a HyPix detector
Radiation source: micro-focus sealed X-ray tube, PhotonJet (Cu) X-ray Source
Mirror monochromator
ω scans
Absorption correction: gaussian (CrysAlis PRO; Rigaku OD, 2018)
$T_{min} = 0.300$, $T_{max} = 1.000$
37979 measured reflections
5613 independent reflections
5268 reflections with $I > 2\sigma(I)$
$R_{int} = 0.039$
$\theta_{max} = 66.5°$, $\theta_{min} = 2.8°$
$h = -9\rightarrow 8$
$k = -15\rightarrow 15$
$l = -33\rightarrow 37$

Refinement

Refinement on F^2
Least-squares matrix: full
$R[F^2 > 2\sigma(F^2)] = 0.028$
$wR(F^2) = 0.070$
$S = 1.02$
5613 reflections
486 parameters
0 restraints
Hydrogen site location: inferred from neighbouring sites
H-atom parameters constrained
$w = 1/[\sigma^2(F_o^2) + (0.0314P)^2 + 3.2601P]$ where $P = (F_o^2 + 2F_c^2)/3$
$(\Delta/\sigma)_{max} = 0.001$
$\Delta\rho_{max} = 0.60$ e Å^{-3}
$\Delta\rho_{min} = -0.77$ e Å^{-3}

Special details

Geometry. All e.s.d.'s (except the e.s.d. in the dihedral angle between two l.s. planes) are estimated using the full covariance matrix. The cell e.s.d.'s are taken into account individually in the estimation of e.s.d.'s in distances, angles and torsion angles; correlations between e.s.d.'s in cell parameters are only used when they are defined by crystal symmetry. An approximate (isotropic) treatment of cell e.s.d.'s is used for estimating e.s.d.'s involving l.s. planes.

Fractional atomic coordinates and isotropic or equivalent isotropic displacement parameters (Å²)

	x	*y*	*z*	U_{iso}*/U_{eq}	Occ. (<1)
Se1	0.65737 (3)	0.42578 (2)	0.43767 (2)	0.03035 (8)	
Se2	0.65188 (3)	0.64005 (2)	0.34377 (2)	0.03505 (8)	
N1	0.5833 (2)	0.20696 (14)	0.44266 (6)	0.0270 (4)	
N2	0.3857 (2)	0.29649 (13)	0.40949 (5)	0.0228 (4)	
N3	0.3914 (2)	0.53847 (14)	0.29349 (5)	0.0250 (4)	
N4	0.5899 (2)	0.60572 (14)	0.25347 (6)	0.0277 (4)	
C1	0.7135 (4)	0.4171 (2)	0.49873 (8)	0.0433 (6)	
H1A	0.620462	0.381536	0.513578	0.065*	
H1AB	0.726361	0.485887	0.510494	0.065*	
H1AC	0.821774	0.379496	0.502677	0.065*	
C2	0.4748 (4)	0.7348 (3)	0.36256 (10)	0.0541 (7)	
H2A	0.512508	0.767708	0.389198	0.081*	
H2AB	0.367043	0.697746	0.367425	0.081*	
H2AC	0.455801	0.786789	0.340499	0.081*	
C3	0.5385 (3)	0.30088 (16)	0.43047 (6)	0.0244 (4)	
C4	0.7418 (3)	0.1769 (2)	0.46527 (9)	0.0439 (6)	
H4A	0.719025	0.171376	0.495941	0.066*	
H4AB	0.831422	0.228253	0.460559	0.066*	
H4AC	0.781135	0.110890	0.454429	0.066*	
C5	0.4536 (3)	0.13950 (17)	0.43035 (7)	0.0286 (5)	
C6	0.4380 (4)	0.03435 (18)	0.43572 (8)	0.0382 (6)	
H6	0.522600	−0.004595	0.450651	0.046*	
C7	0.2925 (4)	−0.0094 (2)	0.41803 (9)	0.0466 (7)	
H7	0.276908	−0.080869	0.420733	0.056*	
C8	0.1666 (4)	0.0474 (2)	0.39622 (9)	0.0451 (7)	
H8	0.068092	0.013546	0.384810	0.054*	
C9	0.1819 (3)	0.15228 (19)	0.39078 (8)	0.0350 (5)	
H9	0.097531	0.191347	0.375827	0.042*	
C10	0.3293 (3)	0.19581 (16)	0.40876 (7)	0.0263 (4)	
C11	0.5374 (3)	0.59428 (17)	0.29369 (7)	0.0259 (4)	
C12	0.7436 (3)	0.6609 (2)	0.23925 (9)	0.0418 (6)	
H12A	0.789534	0.702111	0.262879	0.063*	
H12B	0.712557	0.705366	0.215211	0.063*	
H12C	0.831466	0.611974	0.230146	0.063*	
C13	0.4767 (3)	0.55470 (16)	0.22628 (7)	0.0274 (4)	
C14	0.4739 (4)	0.5422 (2)	0.18222 (8)	0.0405 (6)	
H14	0.559900	0.571217	0.164547	0.049*	
C15	0.3396 (4)	0.4855 (2)	0.16546 (8)	0.0467 (7)	
H15	0.332824	0.475704	0.135395	0.056*	
C16	0.2127 (4)	0.4419 (2)	0.19127 (8)	0.0420 (6)	
H16	0.123143	0.402895	0.178266	0.050*	
C17	0.2144 (3)	0.45407 (19)	0.23485 (7)	0.0324 (5)	
H17	0.128460	0.424864	0.252494	0.039*	
C18	0.3495 (3)	0.51175 (16)	0.25161 (6)	0.0252 (4)	
C19	0.3045 (3)	0.38090 (16)	0.38795 (6)	0.0226 (4)	

C20	0.1522 (3)	0.42223 (17)	0.40319 (7)	0.0272 (5)	
H20	0.099529	0.395370	0.428055	0.033*	
C21	0.0786 (3)	0.50337 (19)	0.38142 (7)	0.0318 (5)	
H21	−0.025378	0.532601	0.391576	0.038*	
C22	0.1547 (3)	0.54272 (19)	0.34491 (7)	0.0301 (5)	
H22	0.103140	0.597916	0.329851	0.036*	
C23	0.3072 (3)	0.49972 (17)	0.33100 (6)	0.0246 (4)	
C24	0.3829 (3)	0.41797 (16)	0.35164 (6)	0.0236 (4)	
H24	0.485820	0.388053	0.341198	0.028*	
S2	0.23709 (8)	0.27181 (4)	0.53076 (2)	0.03371 (14)	
F4	0.1481 (3)	0.14818 (19)	0.59164 (7)	0.0915 (8)	
F5	−0.0647 (2)	0.22005 (16)	0.55977 (7)	0.0693 (5)	
F6	0.0696 (3)	0.09949 (15)	0.52938 (9)	0.0915 (7)	
O4	0.2348 (3)	0.35229 (15)	0.56160 (7)	0.0536 (5)	
O5	0.1547 (3)	0.29449 (18)	0.49060 (6)	0.0630 (6)	
O6	0.3970 (3)	0.21663 (19)	0.52873 (7)	0.0632 (6)	
C26	0.0923 (4)	0.1797 (2)	0.55375 (9)	0.0483 (7)	
S1A	0.82979 (10)	0.33445 (8)	0.30604 (3)	0.0304 (3)	0.728 (3)
F1A	0.8104 (4)	0.2125 (2)	0.23925 (10)	0.0611 (8)	0.728 (3)
F2A	0.5919 (5)	0.3100 (3)	0.24631 (12)	0.0580 (9)	0.728 (3)
F3A	0.8292 (3)	0.3715 (2)	0.22338 (7)	0.0585 (7)	0.728 (3)
O1A	0.7200 (5)	0.2707 (3)	0.33147 (13)	0.0531 (9)	0.728 (3)
O2A	1.0134 (13)	0.3105 (6)	0.3063 (2)	0.0341 (11)	0.728 (3)
O3A	0.7920 (3)	0.44154 (19)	0.30852 (10)	0.0446 (7)	0.728 (3)
C27A	0.7659 (14)	0.3056 (8)	0.2506 (3)	0.039 (2)	0.728 (3)
C27B	0.8672 (13)	0.2688 (10)	0.3114 (3)	0.039 (2)	0.272 (3)
O1B	0.7976 (10)	0.4328 (6)	0.2719 (4)	0.069 (3)	0.272 (3)
O2B	0.5834 (15)	0.2999 (10)	0.2679 (4)	0.049 (3)	0.272 (3)
O3B	0.8581 (12)	0.2808 (11)	0.2293 (3)	0.066 (3)	0.272 (3)
F1B	0.7846 (11)	0.2951 (9)	0.3465 (3)	0.070 (3)	0.272 (3)
F2B	1.022 (3)	0.2947 (16)	0.3152 (6)	0.0341 (11)	0.272 (3)
F3B	0.8668 (9)	0.1687 (5)	0.3093 (2)	0.064 (2)	0.272 (3)
S1B	0.7620 (8)	0.3257 (5)	0.26391 (18)	0.0344 (11)	0.272 (3)

Atomic displacement parameters (Å²)

	U^{11}	U^{22}	U^{33}	U^{12}	U^{13}	U^{23}
Se1	0.02959 (13)	0.03091 (14)	0.03050 (13)	−0.00819 (9)	−0.00250 (9)	0.00076 (9)
Se2	0.02722 (14)	0.04291 (16)	0.03488 (14)	−0.00386 (10)	−0.00660 (10)	−0.00055 (10)
N1	0.0296 (9)	0.0268 (9)	0.0246 (9)	0.0009 (7)	0.0010 (7)	0.0016 (7)
N2	0.0228 (8)	0.0257 (9)	0.0200 (8)	−0.0035 (7)	0.0038 (6)	0.0006 (7)
N3	0.0219 (8)	0.0336 (10)	0.0197 (8)	−0.0020 (7)	0.0009 (7)	0.0043 (7)
N4	0.0256 (9)	0.0274 (9)	0.0301 (9)	−0.0024 (7)	0.0068 (7)	0.0040 (7)
C1	0.0525 (16)	0.0437 (15)	0.0334 (13)	−0.0052 (12)	−0.0106 (11)	−0.0058 (11)
C2	0.0454 (16)	0.0613 (19)	0.0554 (17)	0.0049 (14)	−0.0078 (13)	−0.0225 (15)
C3	0.0240 (10)	0.0295 (11)	0.0198 (10)	−0.0018 (8)	0.0029 (8)	0.0000 (8)
C4	0.0410 (14)	0.0407 (14)	0.0498 (15)	0.0086 (11)	−0.0116 (12)	0.0033 (12)
C5	0.0349 (12)	0.0283 (11)	0.0228 (10)	−0.0029 (9)	0.0087 (9)	−0.0016 (8)

C6	0.0532 (15)	0.0289 (12)	0.0327 (12)	−0.0001 (11)	0.0138 (11)	0.0031 (10)
C7	0.0620 (17)	0.0290 (13)	0.0492 (15)	−0.0147 (12)	0.0215 (13)	−0.0035 (11)
C8	0.0452 (15)	0.0422 (14)	0.0482 (15)	−0.0210 (12)	0.0125 (12)	−0.0110 (12)
C9	0.0325 (12)	0.0395 (13)	0.0332 (12)	−0.0090 (10)	0.0075 (10)	−0.0061 (10)
C10	0.0296 (11)	0.0268 (11)	0.0226 (10)	−0.0064 (9)	0.0096 (8)	−0.0015 (8)
C11	0.0220 (10)	0.0289 (11)	0.0267 (11)	0.0017 (8)	0.0014 (8)	0.0027 (9)
C12	0.0363 (13)	0.0434 (14)	0.0460 (14)	−0.0139 (11)	0.0154 (11)	0.0029 (11)
C13	0.0317 (11)	0.0250 (11)	0.0255 (11)	−0.0002 (9)	0.0056 (9)	0.0023 (8)
C14	0.0541 (15)	0.0412 (14)	0.0265 (12)	−0.0077 (12)	0.0131 (11)	0.0019 (10)
C15	0.0673 (18)	0.0500 (16)	0.0229 (12)	−0.0142 (14)	0.0064 (11)	−0.0045 (11)
C16	0.0533 (16)	0.0437 (14)	0.0290 (12)	−0.0132 (12)	−0.0018 (11)	−0.0024 (10)
C17	0.0305 (11)	0.0409 (13)	0.0258 (11)	−0.0066 (10)	0.0009 (9)	0.0059 (9)
C18	0.0275 (10)	0.0281 (11)	0.0201 (10)	0.0016 (9)	0.0020 (8)	0.0040 (8)
C19	0.0214 (10)	0.0275 (11)	0.0190 (9)	−0.0038 (8)	0.0001 (8)	−0.0016 (8)
C20	0.0227 (10)	0.0388 (12)	0.0201 (10)	−0.0024 (9)	0.0039 (8)	0.0012 (9)
C21	0.0223 (10)	0.0454 (13)	0.0278 (11)	0.0054 (10)	0.0055 (8)	0.0009 (10)
C22	0.0239 (11)	0.0394 (13)	0.0269 (11)	0.0032 (9)	−0.0015 (9)	0.0040 (9)
C23	0.0216 (10)	0.0342 (11)	0.0181 (10)	−0.0054 (9)	0.0017 (8)	0.0015 (8)
C24	0.0180 (9)	0.0319 (11)	0.0209 (10)	−0.0011 (8)	0.0020 (8)	0.0000 (8)
S2	0.0418 (3)	0.0356 (3)	0.0239 (3)	−0.0108 (2)	0.0078 (2)	−0.0002 (2)
F4	0.0806 (14)	0.1174 (18)	0.0760 (14)	−0.0289 (13)	−0.0233 (11)	0.0721 (14)
F5	0.0361 (9)	0.0898 (14)	0.0821 (13)	−0.0170 (9)	0.0008 (8)	0.0215 (11)
F6	0.1023 (17)	0.0403 (10)	0.131 (2)	−0.0263 (11)	−0.0255 (15)	−0.0046 (12)
O4	0.0619 (13)	0.0463 (11)	0.0525 (12)	−0.0137 (9)	0.0055 (9)	−0.0187 (9)
O5	0.0956 (17)	0.0673 (14)	0.0263 (9)	−0.0012 (12)	0.0000 (10)	0.0162 (9)
O6	0.0446 (11)	0.0844 (16)	0.0609 (13)	0.0016 (11)	0.0140 (10)	−0.0131 (12)
C26	0.0465 (16)	0.0443 (16)	0.0538 (16)	−0.0142 (12)	−0.0152 (12)	0.0205 (13)
S1A	0.0247 (4)	0.0284 (6)	0.0381 (5)	0.0023 (3)	0.0045 (3)	−0.0052 (3)
F1A	0.0574 (16)	0.0514 (15)	0.0745 (18)	−0.0056 (13)	0.0013 (13)	−0.0349 (14)
F2A	0.0324 (14)	0.0642 (19)	0.077 (2)	−0.0109 (12)	−0.0141 (19)	−0.013 (2)
F3A	0.0561 (15)	0.0740 (19)	0.0452 (13)	−0.0226 (14)	−0.0094 (11)	0.0064 (12)
O1A	0.046 (2)	0.0530 (18)	0.060 (2)	−0.0061 (16)	0.0217 (17)	0.0019 (17)
O2A	0.0296 (13)	0.033 (3)	0.040 (4)	0.0034 (18)	0.003 (2)	0.0030 (18)
O3A	0.0425 (14)	0.0325 (13)	0.0587 (18)	0.0090 (11)	−0.0093 (13)	−0.0168 (12)
C27A	0.034 (3)	0.037 (4)	0.046 (5)	−0.005 (3)	−0.001 (4)	−0.010 (3)
C27B	0.046 (6)	0.040 (7)	0.031 (5)	0.014 (5)	−0.016 (4)	−0.006 (4)
O1B	0.038 (4)	0.031 (4)	0.136 (10)	0.002 (3)	−0.018 (5)	0.011 (5)
O2B	0.026 (4)	0.054 (5)	0.066 (7)	−0.003 (3)	−0.009 (5)	−0.008 (6)
O3B	0.053 (5)	0.117 (12)	0.027 (4)	0.018 (6)	0.002 (4)	−0.022 (5)
F1B	0.045 (5)	0.124 (9)	0.041 (4)	0.017 (5)	0.014 (3)	−0.004 (4)
F2B	0.0296 (13)	0.033 (3)	0.040 (4)	0.0034 (18)	0.003 (2)	0.0030 (18)
F3B	0.059 (4)	0.038 (3)	0.095 (5)	−0.009 (3)	−0.021 (3)	0.018 (3)
S1B	0.0244 (14)	0.034 (2)	0.045 (3)	0.0040 (15)	0.003 (2)	0.0025 (19)

Geometric parameters (Å, º)

Se1—C3	1.893 (2)	C14—C15	1.378 (4)
Se1—C1	1.957 (2)	C14—H14	0.9500

Se2—C11	1.890 (2)	C15—C16	1.401 (4)
Se2—C2	1.948 (3)	C15—H15	0.9500
N1—C3	1.335 (3)	C16—C17	1.372 (3)
N1—C5	1.391 (3)	C16—H16	0.9500
N1—C4	1.465 (3)	C17—C18	1.390 (3)
N2—C3	1.349 (3)	C17—H17	0.9500
N2—C10	1.392 (3)	C19—C24	1.382 (3)
N2—C19	1.438 (3)	C19—C20	1.388 (3)
N3—C11	1.348 (3)	C20—C21	1.384 (3)
N3—C18	1.391 (3)	C20—H20	0.9500
N3—C23	1.441 (3)	C21—C22	1.390 (3)
N4—C11	1.335 (3)	C21—H21	0.9500
N4—C13	1.388 (3)	C22—C23	1.384 (3)
N4—C12	1.467 (3)	C22—H22	0.9500
C1—H1A	0.9800	C23—C24	1.380 (3)
C1—H1AB	0.9800	C24—H24	0.9500
C1—H1AC	0.9800	S2—O4	1.4308 (19)
C2—H2A	0.9800	S2—O5	1.434 (2)
C2—H2AB	0.9800	S2—O6	1.437 (2)
C2—H2AC	0.9800	S2—C26	1.804 (3)
C4—H4A	0.9800	F4—C26	1.323 (3)
C4—H4AB	0.9800	F5—C26	1.342 (4)
C4—H4AC	0.9800	F6—C26	1.311 (4)
C5—C10	1.384 (3)	S1A—O3A	1.438 (3)
C5—C6	1.396 (3)	S1A—O1A	1.439 (4)
C6—C7	1.376 (4)	S1A—O2A	1.456 (9)
C6—H6	0.9500	S1A—C27A	1.837 (9)
C7—C8	1.400 (4)	F1A—C27A	1.320 (9)
C7—H7	0.9500	F2A—C27A	1.355 (11)
C8—C9	1.392 (4)	F3A—C27A	1.312 (11)
C8—H8	0.9500	C27B—F2B	1.25 (3)
C9—C10	1.390 (3)	C27B—F3B	1.315 (14)
C9—H9	0.9500	C27B—F1B	1.323 (13)
C12—H12A	0.9800	C27B—S1B	1.844 (12)
C12—H12B	0.9800	O1B—S1B	1.454 (10)
C12—H12C	0.9800	O2B—S1B	1.431 (13)
C13—C14	1.388 (3)	O3B—S1B	1.445 (8)
C13—C18	1.390 (3)		

C3—Se1—C1	99.69 (10)	C13—C14—H14	121.8
C11—Se2—C2	97.32 (11)	C14—C15—C16	122.2 (2)
C3—N1—C5	108.90 (18)	C14—C15—H15	118.9
C3—N1—C4	126.9 (2)	C16—C15—H15	118.9
C5—N1—C4	124.16 (19)	C17—C16—C15	121.7 (2)
C3—N2—C10	108.78 (18)	C17—C16—H16	119.2
C3—N2—C19	124.90 (17)	C15—C16—H16	119.2
C10—N2—C19	126.05 (18)	C16—C17—C18	115.9 (2)
C11—N3—C18	109.19 (17)	C16—C17—H17	122.0

C11—N3—C23	125.12 (17)	C18—C17—H17	122.0
C18—N3—C23	125.06 (17)	C17—C18—C13	122.8 (2)
C11—N4—C13	109.01 (18)	C17—C18—N3	131.26 (19)
C11—N4—C12	126.7 (2)	C13—C18—N3	105.94 (18)
C13—N4—C12	124.24 (19)	C24—C19—C20	121.8 (2)
Se1—C1—H1A	109.5	C24—C19—N2	117.53 (18)
Se1—C1—H1AB	109.5	C20—C19—N2	120.64 (18)
H1A—C1—H1AB	109.5	C21—C20—C19	118.65 (19)
Se1—C1—H1AC	109.5	C21—C20—H20	120.7
H1A—C1—H1AC	109.5	C19—C20—H20	120.7
H1AB—C1—H1AC	109.5	C20—C21—C22	120.9 (2)
Se2—C2—H2A	109.5	C20—C21—H21	119.5
Se2—C2—H2AB	109.5	C22—C21—H21	119.5
H2A—C2—H2AB	109.5	C23—C22—C21	118.5 (2)
Se2—C2—H2AC	109.5	C23—C22—H22	120.7
H2A—C2—H2AC	109.5	C21—C22—H22	120.7
H2AB—C2—H2AC	109.5	C24—C23—C22	122.01 (19)
N1—C3—N2	108.89 (18)	C24—C23—N3	117.49 (18)
N1—C3—Se1	129.86 (16)	C22—C23—N3	120.49 (19)
N2—C3—Se1	121.22 (16)	C23—C24—C19	118.02 (19)
N1—C4—H4A	109.5	C23—C24—H24	121.0
N1—C4—H4AB	109.5	C19—C24—H24	121.0
H4A—C4—H4AB	109.5	O4—S2—O5	115.36 (14)
N1—C4—H4AC	109.5	O4—S2—O6	114.79 (14)
H4A—C4—H4AC	109.5	O5—S2—O6	116.21 (14)
H4AB—C4—H4AC	109.5	O4—S2—C26	102.35 (14)
C10—C5—N1	106.97 (19)	O5—S2—C26	102.44 (13)
C10—C5—C6	121.7 (2)	O6—S2—C26	102.69 (14)
N1—C5—C6	131.3 (2)	F6—C26—F4	108.1 (3)
C7—C6—C5	115.9 (3)	F6—C26—F5	106.4 (2)
C7—C6—H6	122.1	F4—C26—F5	106.6 (3)
C5—C6—H6	122.1	F6—C26—S2	112.8 (2)
C6—C7—C8	122.5 (2)	F4—C26—S2	111.59 (19)
C6—C7—H7	118.8	F5—C26—S2	111.08 (19)
C8—C7—H7	118.8	O3A—S1A—O1A	114.6 (2)
C9—C8—C7	121.8 (2)	O3A—S1A—O2A	114.2 (4)
C9—C8—H8	119.1	O1A—S1A—O2A	117.0 (3)
C7—C8—H8	119.1	O3A—S1A—C27A	101.5 (4)
C10—C9—C8	115.3 (2)	O1A—S1A—C27A	104.3 (4)
C10—C9—H9	122.3	O2A—S1A—C27A	102.3 (5)
C8—C9—H9	122.3	F3A—C27A—F1A	109.6 (7)
C5—C10—C9	122.8 (2)	F3A—C27A—F2A	106.6 (8)
C5—C10—N2	106.42 (19)	F1A—C27A—F2A	106.0 (7)
C9—C10—N2	130.8 (2)	F3A—C27A—S1A	112.2 (6)
N4—C11—N3	108.73 (18)	F1A—C27A—S1A	112.1 (7)
N4—C11—Se2	126.88 (16)	F2A—C27A—S1A	110.0 (5)
N3—C11—Se2	124.28 (15)	F2B—C27B—F3B	106.2 (13)
N4—C12—H12A	109.5	F2B—C27B—F1B	108.7 (13)

N4—C12—H12B	109.5	F3B—C27B—F1B	107.5 (11)
H12A—C12—H12B	109.5	F2B—C27B—S1B	112.5 (10)
N4—C12—H12C	109.5	F3B—C27B—S1B	111.4 (7)
H12A—C12—H12C	109.5	F1B—C27B—S1B	110.4 (8)
H12B—C12—H12C	109.5	O2B—S1B—O3B	118.4 (7)
N4—C13—C14	131.9 (2)	O2B—S1B—O1B	113.3 (7)
N4—C13—C18	107.11 (18)	O3B—S1B—O1B	115.1 (9)
C14—C13—C18	121.0 (2)	O2B—S1B—C27B	104.7 (7)
C15—C14—C13	116.4 (2)	O3B—S1B—C27B	102.1 (6)
C15—C14—H14	121.8	O1B—S1B—C27B	99.9 (7)